OregonWaveEnergy TRUST

Dec 09

Sediment Transport Study

Baseline Observations and Modeling for the Reedsport Wave Energy Site

Prepared by Oregon State University (OSU) and the Oregon Department of Geology and Mineral Industries (DOGAMI) on behalf of Oregon Wave Energy Trust

Oregon Wave Energy Trust (OWET) – with members from fishing and environmental groups, industry and government – is a nonprofit public-private partnership funded by the Oregon Innovation Council in 2007. Its mission is to serve as a connector for all stakeholders involved in wave energy project development – from research and development to early stage community engagement and final deployment and energy generation – positioning Oregon as the North America leader in this nascent industry and delivering its full economic and environmental potential for the state. OWET's goal is to have ocean wave energy producing 2 megawatts of power – enough to power about 800 homes – by 2010 and 500 megawatts of power by 2025.

www.oregonwave.org

Baseline Observations and Modeling for the Reedsport Wave Energy Site

PIs: H.T. Özkan-Haller, J.C. Allan, J.A. Barth, M.C. Haller, R.A. Holman, and P. Ruggiero

This project was carried out collaboratively by Oregon State University (OSU) and the Oregon Department of Geology and Mineral Industries (DOGAMI) and involved baseline observations and modeling at the proposed wave energy conversion (WEC) array site near Reedsport, OR. In particular, observations and predictions of the wave conditions at the proposed site were carried out. Further, a baseline bathymetry survey of the nearshore area shoreward of the site was collected along with regular observations of the topography and shoreline, and video observations of the submerged sand bar features. The observations help characterize the baseline variability at the site and the adjacent beach. Further, the wave observations and predictions inform the wave energy developers about the expected local conditions.

In the following we report on each component of the study. In particular, Appendices A-E contain reports on the beach and shoreline morphodynamics, direct survey as well as video observations of the submerged bathymetry, wave modeling, and in-situ and radar observations of the waves. Below we summarize the overall findings. Finally, we provide recommendations for further monitoring efforts.

OVERALL FINDINGS

Our findings regarding the **morphology of the beach** are summarized below.

- A multiple submerged bar system exists in the surf zone in this area. The nearshore bathymetry survey in July indicates a very straight and parallel sub-tidal outer bar approximately 500 m from the shoreline.
- The bars observed with the video system through Fall 2009 appear highly variable with variability out to 1km from the shoreline. The sand bars also display alongshore variability that is more pronounced during mild wave conditions.
- The bathymetry surveys also indicate the presence of well-resolved mega-ripple features with 20m-length scales and 20cm height and located in 8m water depth. This feature may be indicative of biological activity.
- On the dry beach, sand accumulates in the form of a berm at 2-4m elevation sometime after winter conditions have subsided. The berm is then eroded during the subsequent winter.
- Shoreline position over the 6 months of data collection changed by as much as 70m. Alongshore variability of the shoreline is also on the order ~100m.

Wave modeling and observations indicate the following.

- Typical winter storm conditions at the site consist of swell waves approaching from the southwest at high angles of incidence. Otherwise, waves at the site consist of somewhat lower energy swell approaching directly from the west or northwest and lower period waves approaching from the northwest. Note that the direction of approach of the winter swells can vary significantly during an El Niño or La Niña year.

- The most pronounced bathymetric features in this area are the Stonewall and Heceta Banks that have the potential of focusing wave energy, and Cape Blanco that has the potential of shielding the shoreline near the WEC array site from southern wave energy.
- Wave model simulations suggest that low period waves from the north are minimally affected by the bank systems and that the effect of the banks on long period swell waves is most pronounced to the north of the proposed WEC array site. Hence, the WEC array site is not affected significantly by the bank systems.
- The simulations also suggest that Cape Blanco may have a significant effect on the waves at the WEC site. Consequently, during periods of swell waves from the southwest conditions at the WEC site may be associated with less energetic and less oblique waves (compared to observations at deep water buoys).
- Observations of wave characteristics at the WEC array site support the hypothesis that Cape Blanco is influencing the waves at the site, because the observations also indicate lower wave heights and smaller angles of incidence at the site (compared to the deep water buoy) when wave incidence is from the southwest.
- Radar observations of the waves are consistent with in situ observations and demonstrated shipboard wave observing capabilities that can be used at the WEC site.

Preliminary numerical simulations of the potential effect of a WEC array on the wave height in the area were also carried out and indicate the following.

- Wave height variations up to 15% are possible immediately in the lee of an array with length scales of variability similar to the distances between the individual devices. This variability is significantly smoothed at distances ~1km from the array. Far-field effects are confined to about 3% variability in the wave height.
- These results are very preliminary and must be calibrated and validated using observation of the shadow region around an actual buoy. We note that the details of the shadow regions may also be a function of the particular design of a structure.

RECOMMENDATIONS FOR FUTURE MONITORING

- The regular observations of shoreline and beach variability have so far only covered a 6-month period. Hence, in its current form the data set is of limited value, in part because it does not cover the winter and spring months when many storm-related changes occur. Further, avoiding gaps in the observations will ensure a full view at the background variability at the site. The continuation of these observations is crucial to capability of the resulting data set to fully characterize background variability.
- Our understanding is that OPT will at first deploy one WEC device in the summer of 2010. We strongly recommend that wave observations are carried out in the vicinity of this buoy. In particular, in situ and radar observations will help us determine the nature of the shadow zone behind the buoy. These observations are crucial to the calibration and verification of the preliminary modeling that is aimed at predicting the effects of an array of WEC devices on the surrounding near-field wave conditions so that potential effects on the neighboring shorelines can be assessed.
- Once OPT's WEC array is installed, the wave, bathymetry and shoreline observations should still continue so that the effects of the buoy field can be distinguished from background variability at the site.

Appendix A

Monitoring Beach and Shoreline Morphodynamics

Jonathan Allan
Oregon Department of Geology and Mineral Industries

Background

The wave climate offshore of the Pacific Northwest (PNW) coasts of Oregon and Washington has been identified as an ideal environment for the establishment of wave energy devices that can be used to harness the energy potential provided by ocean waves. Since wave energy arrays by definition will remove a portion of the energy of the waves and will create a shadow region of lower wave energy landward of the arrays, there remain concerns about the potential effects such devices may have on the morphodynamics of beaches adjacent to wave energy farms. To understand the effects of wave energy arrays on sediment transport processes, a collaborative team of investigators from Oregon State University (OSU) and the Oregon Department of Geology & Mineral Industries (DOGAMI) initiated a field-based monitoring program in May 2009 in order to begin documenting the natural variability of the beach, nearshore and wave climate adjacent to the proposed Reedsport wave energy site. This report describes preliminary findings from one component of the observation program focused on monitoring the response of the beach and shorelines along approximately 16 km of the North Umpqua Spit shoreline.

Methodology

Approaches for Monitoring Beaches

Beach profiles that are orientated perpendicular to the shoreline can be surveyed using a variety of approaches, including a simple graduated rod and chain, surveying level and staff, Total Station theodolite and reflective prism, Light Detection and Ranging (LIDAR) airborne altimetry, and Real-Time Kinematic Differential Global Positioning System (RTK-DGPS) technology. Traditional techniques such as leveling instruments and Total Stations are capable of providing accurate representations of the morphology of a beach, but are demanding in terms of time and effort. At the other end of the spectrum, high-resolution topographic surveys of the beach derived from LIDAR are ideal for capturing the 3-dimensional state of the beach, over an extended length of coast within a matter of hours; other forms of LIDAR technology are now being used to measure nearshore bathymetry out to moderate depths, but are dependent on water clarity. However, the LIDAR technology remains expensive and is impractical along small segments of shore, and more importantly, the high costs effectively limits the temporal resolution of the surveys and hence the ability of the end-user to understand short-term changes in the beach morphology (Bernstein et al., 2003).

Within the range of surveying technologies, the application of RTK-DGPS for surveying the morphology of both the sub-aerial and sub-aqueous portions of the beach has effectively become the accepted standard (Allan and Hart, 2007; Bernstein et al., 2003; Ruggiero et al., 2005), and has been the surveying technique used in this study. The global Positioning System (GPS) is a worldwide radio-navigation system formed from a constellation of 30 satellites and their ground stations, originally developed by the Department of Defense. In its simplest form, GPS can be thought of as triangulation with the GPS satellites acting as reference points, enabling users to calculate their position to within several meters (e.g. off the shelf hand-held units), while survey grade GPS units are capable of providing positional and elevation measurements that are

accurate to a centimeter. At least four satellites are needed mathematically to determine an exact position, although more satellites are generally available. The process is complicated since all GPS receivers are subject to error, which can significantly degrade the accuracy of the derived position. These errors include the GPS satellite orbit and clock drift plus signal delays caused by the atmosphere and ionosphere and multipath effects (where the signals bounce off features and create a poor signal). For example, hand-held autonomous receivers have positional accuracies that are typically less than about 10 m (<~30 ft), but can be improved to less than 5 m (<~15 ft) using the Wide Area Augmentation System (WAAS). This latter system is essentially a form of differential correction that accounts for the above errors, which is then broadcast through one of two geostationary satellites to WAAS enabled GPS receivers.

Greater survey accuracies are achieved with differential GPS (DGPS) using two or more GPS receivers to simultaneously track the same satellites enabling comparisons to be made between two sets of observations. One receiver is typically located over a known reference point and the position of an unknown point is determined relative to that reference point. With the more sophisticated 24-channel dual-frequency RTK-DGPS receivers, positional accuracies can be improved to the sub-centimeter level when operating in static mode and to within a few centimeters when in RTK mode (i.e. as the rover GPS is moved about). In this study we used a Trimble© 24-channel dual-frequency 5700/5800 GPS, which consists of a GPS base station (5700 unit), Zephyr Geodetic antenna, HPB450 radio modem, and 5800 "rover" GPS (Figure A1). Trimble reports that the 5700/5800 GPS system have horizontal errors of approximately ±1-cm + 1ppm (parts per million * the baseline length) and ±2-cm in the vertical (Trimble, 2005).

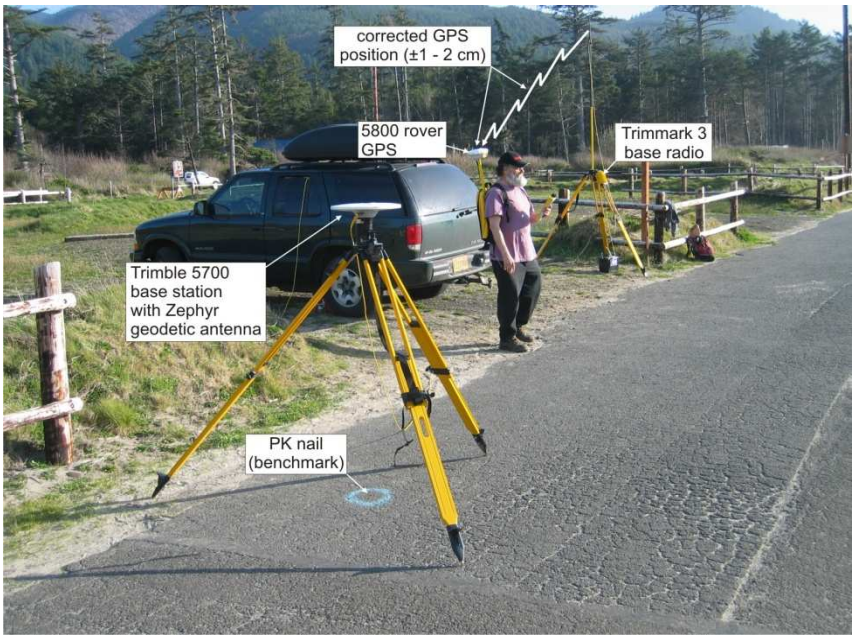

Figure A1 The Trimble 5700 base station antenna located over a known reference point at Cape Lookout State Park. Corrected GPS position and elevation information is then transmitted by a radio modem to the 5800 GPS rover unit.

To convert a space-based positioning system to a ground-based local grid coordinate system, a precise mathematical transformation is necessary. While some of these adjustments are

accomplished by specifying the map projection, datum and geoid model prior to commencing a field survey, an additional transformation is necessary whereby the GPS measurements are tied to known ground control points. This latter step is called a GPS site calibration, such that the GPS measurements are calibrated to ground control points with known vertical and horizontal coordinates using a rigorous least-squares adjustments procedure. Performing the calibration is initially undertaken in the field using the Trimble TSC2 GPS controller and then re-evaluated in the office using Trimble's Geomatics Office software. However, in order to undertake such a transformation, it is necessary to either locate pre-existing monuments used by surveyors or establish new monuments in the project area that can be tied to an existing survey network.

Survey Benchmarks and GPS Control

In order to establish a dense GPS beach monitoring network, we initially identified the approximate locations of the profile sites used in this study in a Geographical Information System (GIS). A reconnaissance trip was undertaken in late April 2009 with the objectives being:

1. To locate existing survey benchmarks in the vicinity of the field site;
2. Field check potential new survey benchmark locations and install these in the vicinity of the beach; and,
3. Layout and initiate the first survey of the beach monitoring network.

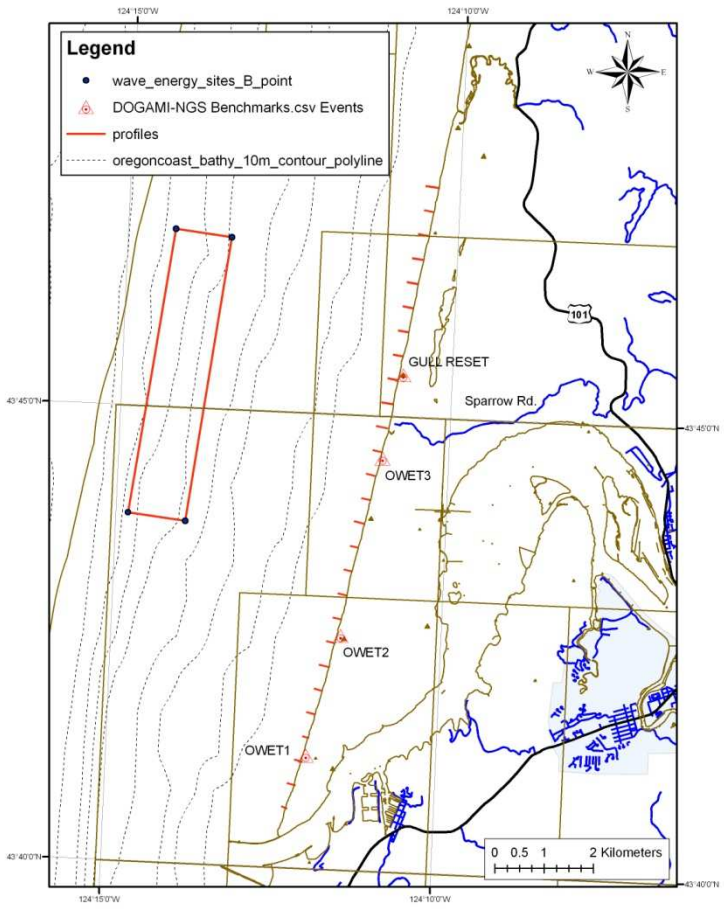

Figure A2 Map showing the location of the study site, beach monitoring network, and DOGAMI survey monuments.

Figure A2 shows the general layout of the final survey network, which consists of 26 profiles sites spaced approximately 500 m apart and extending from the north Umpqua jetty in the south to Tahkenitch Creek in the north, and three permanently monumented survey benchmarks established by DOGAMI that would serve as GPS control for the beach profile surveys, bathymetry survey, and rectification of the ARGUS video imagery. The benchmarks (OWET 1-3) were installed on April 26th, 2009 and were constructed by first digging 1 m deep (10" diameter) holes, into which aluminum sectional rods were inserted and hammered to additional depths of approximately 4 – 8 m (12 - 24 ft, Figure A2). The rods were then capped with a 2½" aluminum cap (Oregon Department of Geology and Mineral Industries stamping on top), and concreted in place.

Survey control along the North Umpqua Spit shore was initially established by occupying two Watershed Sciences benchmarks[1] and one National Geodetic Survey monument. Additional survey control and field checking was provided using the Online Positioning User Service (OPUS) maintained by the NGS (http://www.ngs.noaa.gov/OPUS/). OPUS provides a simplified way to access high-accuracy National Spatial Reference System (NSRS) coordinates using a network of continuously operating GPS reference stations (CORS, http://www.ngs.noaa.gov/CORS/). In order to use OPUS, static GPS measurements are typically made using a fixed height tripod for periods of 2 hours or greater. OPUS returns a solution report with positional accuracy confidence intervals for adjusted coordinates and elevations for the observed point. In all cases we used the Oregon State Plane coordinate system, southern zone (meters), while the vertical datum is relative to the North American Vertical Datum of 1988 (NAVD88).

Table A1 Survey benchmarks used to initially calibrate GPS surveys of the beach near Reedsport. Asterisk signifies the location of the GPS base station during each respective survey. NGS denotes National Geodetic survey monument, WS denotes Watershed Sciences monument.

Name	Northing (m)	Easting (m)	Elevation (m)
6NCM2 - WS	232574.125	1209536.395	5.498
6NCM1 - WS	257724.630	1215506.527	66.410
SOOS - NGS	252644.942	1209669.065	5.500

For the initial Reedsport survey, the 5700 GPS base station was located on the OWET1 monument (Figure A2) using a 2.0 m fixed height tripod. Survey control was provided by undertaking 180 GPS epoch measurements (~ 3 minutes of measurement per calibration site) using the three control sites identified in Table A1, enabling us to perform a GPS site calibration which brought the survey into a local coordinate system. This step is critical in order to eliminate various survey errors that may be compounded by factors such as poor satellite geometry, multipath, and poor atmospheric conditions, combining to increase the total error to several centimeters. In addition, because the 5700 GPS base station was located on each of the OWET (1-3) benchmarks for several hours (typically 2- 6 hours, over multiple days), the

[1] As part of calibrating the collection of Light Detection and Ranging (Lidar) data on the southern Oregon coast in 2008, Watershed Sciences established numerous survey monuments on the south coast. Coordinates assigned to these monuments were derived from multi-hour occupations of the monuments and were processed using the Online Positioning User Service (OPUS) maintained by the NGS. (http://www.ngs.noaa.gov/OPUS/). In many cases, the same benchmarks were observed multiple times and the horizontal and vertical coordinates were continually updated.

measured GPS data from the base station and rover GPS were able to be submitted to OPUS for online processing. Table A2 shows the final derived coordinates assigned to the three benchmarks and their relative uncertainty based on multiple occupations. It is these final coordinates that are used to perform a GPS site calibration each time a field survey of the beach and shoreline is performed.

Table A2 Final coordinates and elevations derived for the three DOGAMI OWET benchmarks established on the north Umpqua Spit. The variance reflects the standard deviation derived from multiple occupations.

	OWET 1 (m)	variance (± m)	OWET 2	variance (± m)	OWET 3	variance (± m)
Northing	231039.181	*0.004*	233473.260	*0.003*	1203406.530	*0.003*
Easting	1201842.604	*0.014*	1202548.920	*0.004*	237078.110	*0.004*
Elevation	8.416	*0.011*	11.629	*0.005*	9.184	*0.039*

Beach Monitoring

Having performed a GPS site calibration, cross-shore beach profiles are surveyed with the 5800 GPS rover unit mounted on a backpack, worn by a surveyor (Figure A3). This was undertaken during periods of low tide, enabling more of the beach to be surveyed. The approach was to generally walk from the landward edge of the primary dune or bluff edge, down the beach face and out into the ocean to approximately wading depth. A straight line, perpendicular to the shore was achieved by navigating along a pre-determined line displayed on a hand-held Trimble TSC2 computer controller, connected to the 5800 rover. The computer shows the position of the operator relative to the survey line and indicates the deviation of the GPS operator from the line. The horizontal variability during the survey is generally minor, being typically less than about ±0.25 m either side of the line, which results in negligible vertical uncertainties due to the relatively uniform nature of beaches characteristic of much of the Oregon coast (Ruggiero et al., 2005). Based on our previous research at numerous sites along the Oregon coast , this method of surveying can reliably detect elevation changes on the order of 4-5 cm, that is well below normal seasonal changes in beach elevation, which typically varies by 1 - 2 m (3 - 6ft) (Allan and Hart, 2007; Allan and Hart, 2008).

Figure A3 Surveying the morphology of the beach at Bandon using a Trimble 5800 'rover' GPS.

Analysis of the beach survey data involved a number of stages. The data was first imported into MATLAB[2] using a customized script. A least-square linear regression was then fit to the profile data. The purpose of this script is to examine the reduced data and eliminate those data point residuals that exceed a ±0.5 m threshold (i.e. the outliers) either side of the predetermined profile line. The data is then exported into an EXCEL database for archiving purposes. A second MATLAB script takes the EXCEL profile database and plots the survey data (relative to the earlier surveys) and outputs the generated figure as a Portable Network Graphics file (Figure A4). These data have been subsequently uploaded to the Oregon Beach and Shoreline Mapping and Analysis (OBSMAP) website maintained by DOGAMI for easy viewing and can be accessed using the following link: http://www.oregongeology.org/sub/Nanoos1/Beach%20profiles/OWET_Cell.htm.

[2] Computer programming languages.

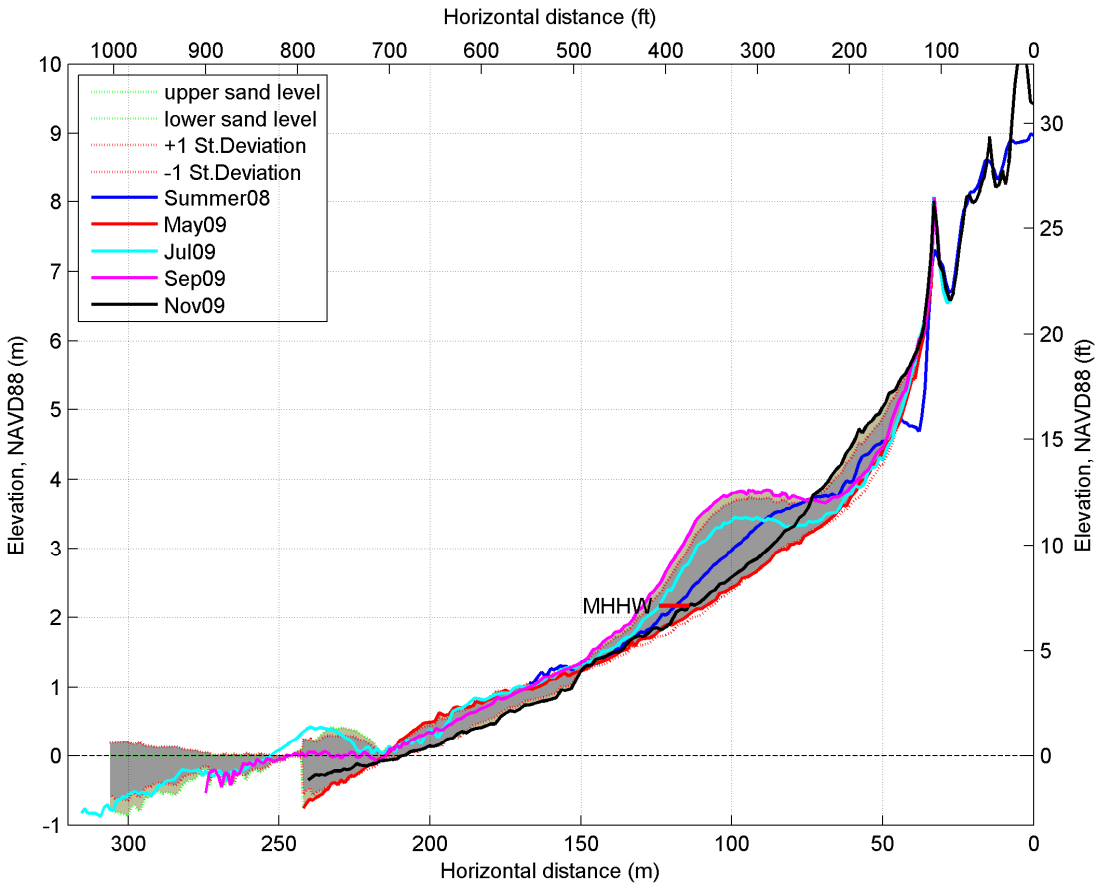

Figure A4 Example of beach profile changes determined at the Reedsport 15 beach profile site. Grey shading denotes the maximum and minimum beach changes (excluding the Lidar data), while the dark grey shading indicates the typical range of variability determined as ± 1 standard deviation about the mean profile. As more beach change information is collected, the dark grey shading will be constrained further and will provide an indication of the normal expected ranges of response. Note the accumulation of sand as a berm between the 2-4 m elevation contours, which reflects the normal post winter aggradation of the beach.

Table A3 indicates the dates when field surveys were performed. At the time of writing, measurements of the morphology of the beach and shoreline have been made on four occasions. To supplement the GPS beach survey data and to extend the time series, Light Detection and Ranging (Lidar) data measured by Watershed Sciences in summer 2008 for DOGAMI were also examined and integrated into the beach profile dataset.

Table A3 Beach Profile Survey Date
27 - 28 April
6 - 9 July
17 - 19 September
17 - 18 November

Shoreline Changes

While beach profiles provide important information about the cross-shore and to some degree the longshore response of the beach as a result of variations in the incident wave energy, nearshore currents, tides, and sediment supply, it is also necessary to understand the alongshore variability in shoreline response that may reflect the development of large morphodynamic features such as rip embayments, beach cusps, and the alongshore transport of sediment. To complement the beach profile surveys initiated along the Umpqua Spit, surveys of a tidal datum-based shoreline were also undertaken. For the purposes of this study we used the Mean Higher High Water tidal datum measured at the Charleston tide gauge as a shoreline proxy and is located at an elevation of 2.17 m NAVD88. Measurement of the shoreline was undertaken by mounting the rover 5800 GPS on to the side of a vehicle and driving two lines above and below the MHHW contour in order to bracket the shoreline. The GPS data were then gridded in a Geographical Information System (GIS) in order to extract the 2.17 m shoreline proxy. Figure A5 shows the locations of selected shoreline positions measured between April and November 2009. Apparent from the plot is the degree of alongshore variability in the shoreline positions, which range from crosshore excursions as low as 10 m to as much as 70 m adjacent to the creek. Aside from these contemporary shorelines, additional shorelines have been obtained from National Ocean Service Topographic "T" sheets for the 1920s and 1950s, as well as from aerial photographs of the coast further extending the time history of shoreline responses for this area.

Summary

In April 2009, DOGAMI staff installed a beach monitoring program to assist with characterizing the baseline level of beach variability along the north Umpqua Spit and especially landward of the proposed Reedsport wave energy array. Over the past 6 months, DOGAMI has collected a total of 104 beach profile surveys along the spit and derived multiple shorelines. In addition, DOGAMI staff have assisted colleagues at OSU in providing survey control for the collection of nearshore bathymetry and ARGUS video images of the nearshore. Over time as more data is collected and synthesized, an improved understanding of the natural level of beach and shoreline morphodynamics will be gained, proving researchers with the necessary information to better characterize any potential future effects to the beach system in response to the installation of wave energy arrays.

References

Allan, J.C. and Hart, R., 2007. Assessing the temporal and spatial variability of coastal change in the Neskowin littoral cell: Developing a comprehensive monitoring program for Oregon beaches Open-file-report O-07-01, Oregon Department of Geology and Mineral Industries, Portland, Oregon.

Allan, J.C. and Hart, R., 2008. Oregon beach and shoreline mapping and analysis program: 2007-2008 beach monitoring report. Open file report O-08-15, Oregon Department of Geology and Mineral Industries, Portland.

Bernstein, D.J. et al., 2003. Survey design analysis for three-dimensional mapping of beach and nearshore morphology, Coastal Sediments '03. American Society of Civil Engineers, St. Peterburgh, Florida, pp. 12.

Ruggiero, P., Kaminsky, G.M., Gelfenbaum, G. and Voight, B., 2005. Seasonal to interannual morphodynamics along a high-energy dissipative littoral cell. Journal of Coastal Research, 21(3): 553-578.

Trimble, 2005. Trimble 5700 GPS system Datasheet, Trimble Navigation Limited, Dayton, Ohio.

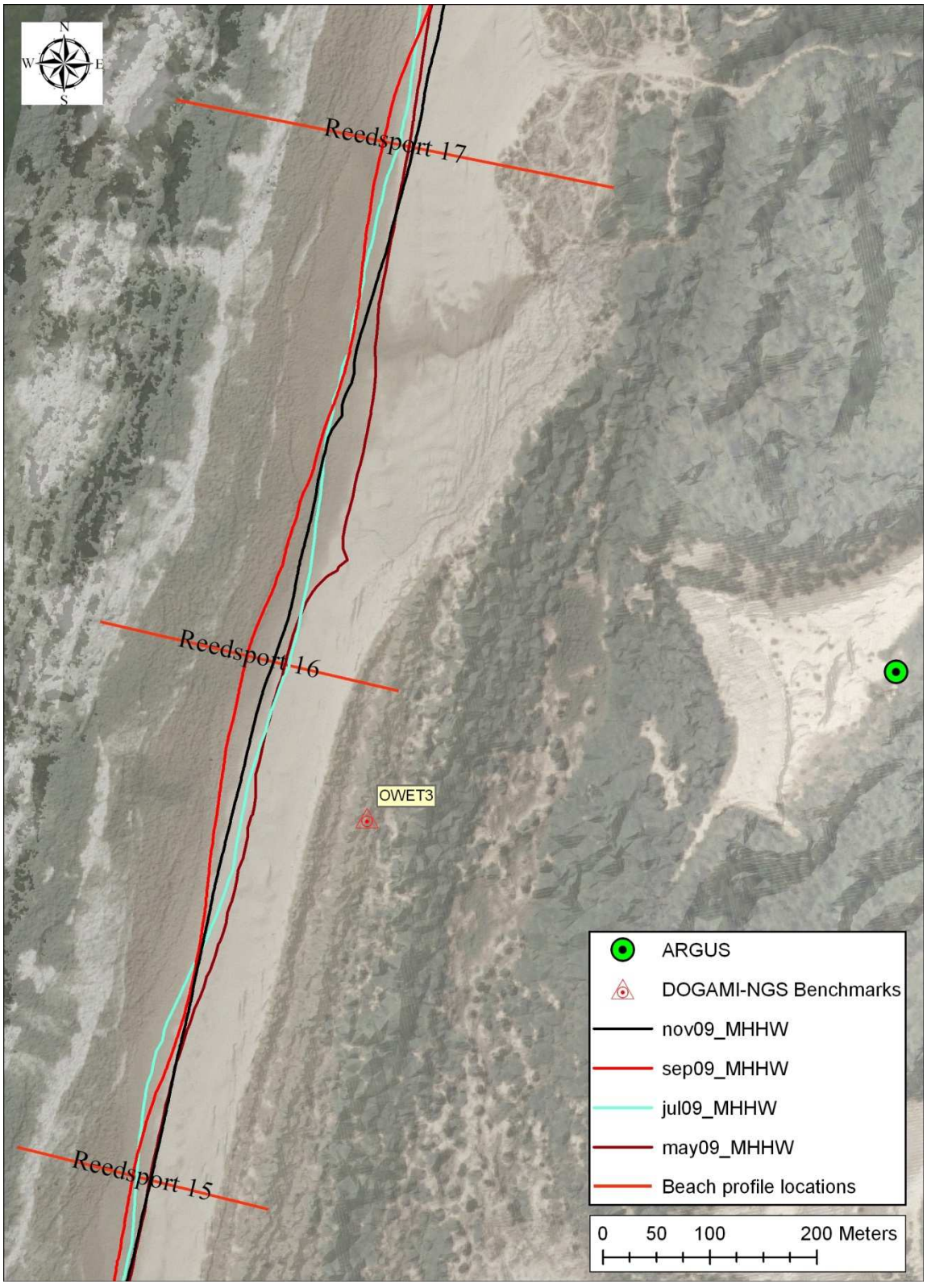

Figure A5 Map showing the locations of selected shoreline positions measured between April and November 2009.

Appendix B

Nearshore Bathymetry Survey
Peter Ruggiero
Oregon State University

Between the dates of 6-10 July 2009 Oregon State University performed a nearshore bathymetric survey along the beaches immediately north of the Winchester Bay North Jetty using the Coastal Profiling System (high-speed maneuverable personal water-craft (PWC) equipped with an echo-sounder and Global Positioning System, see Figure B1) . The primary goals of this work were to assess baseline nearshore morphological conditions along the study site and to provide necessary data for the wave modeling effort described elsewhere in this report.

Our field team consisted of Dr. Peter Ruggiero, Justin Broderson and graduate students, Erica Harris, Jeremy Mull, and Heather Baron. The survey consisted of 45 cross-shore transects extending from between 2 to 4 km offshore to approximately 1-2 m water depth in the surf zone. Topographic data was collected synoptically with the bathymetry data by Jon Allan of DOGAMI to enable a complete mapping of the nearshore planform.

Field Equipment and Data Quality

The Coastal Profiling System (CPS), mounted on a Personal Watercraft (PWC), consists of a single beam echo sounder, GPS receiver and antenna, and an onboard computer (Figure B1). This system is capable of measuring water depths from approximately 0.5*m* to approximately 100*m*. The survey-grade GPS equipment to be used in this project have manufacturer reported RMS accuracies of approximately ±3*cm* + 2ppm of baseline length (typically 10*km* or less) in the horizontal and approximately ±5*cm* + 2ppm in the vertical while operating in Real Time Kinematic surveying mode. These reported accuracies are, however, additionally subject to multi-path, satellite obstructions, poor satellite geometry, and atmospheric conditions that can combine to cause a vertical GPS drift that can be as much as 10*cm*.

While the horizontal uncertainty of individual data points is approximately 0.05*m*, the CPS operators cannot stay “on line,” in waves and currents, to this level of accuracy. Typically, mean offsets are less than 2.0*m* from the preprogrammed track lines and maximum offsets along the approximately 2*km* long transects are typically less than 10.0*m*. While repeatability tests and merges with topographic data collected with an all-terrain survey vehicle or a backpack suggest sub-decimeter vertical accuracy significant variability in seawater temperature (~10 degrees Celsius) can affect depth estimates by as much as 20*cm* in 12*m* of water. However, water temperatures usually remain within a few degrees of the temperature associated with the preset sound velocity estimate and attempts are made to correct for variations in sound velocity. Therefore, a conservative estimate of the total vertical uncertainty for these nearshore bathymetry measurements is approximately 0.15*m*.

For more information regarding equipment, field techniques, and data quality please refer to the following:

Ruggiero, P., Eshleman, J., Kingsley, E., Kaminsky, G., Thompson, D.M , Voigt, B., Kaminsky, G., and Gelfenbaum, G., 2007. Beach monitoring in the Columbia River littoral cell: 1997-2005., U. S. Geological Survey Data Series 260.

Ruggiero, P., Kaminsky, G.M., Gelfenbaum, G., and Voigt, B., 2005. Seasonal to interannual morphodynamics along a high-energy dissipative littoral cell, *Journal of Coastal Research*, 21(3), 553-578.

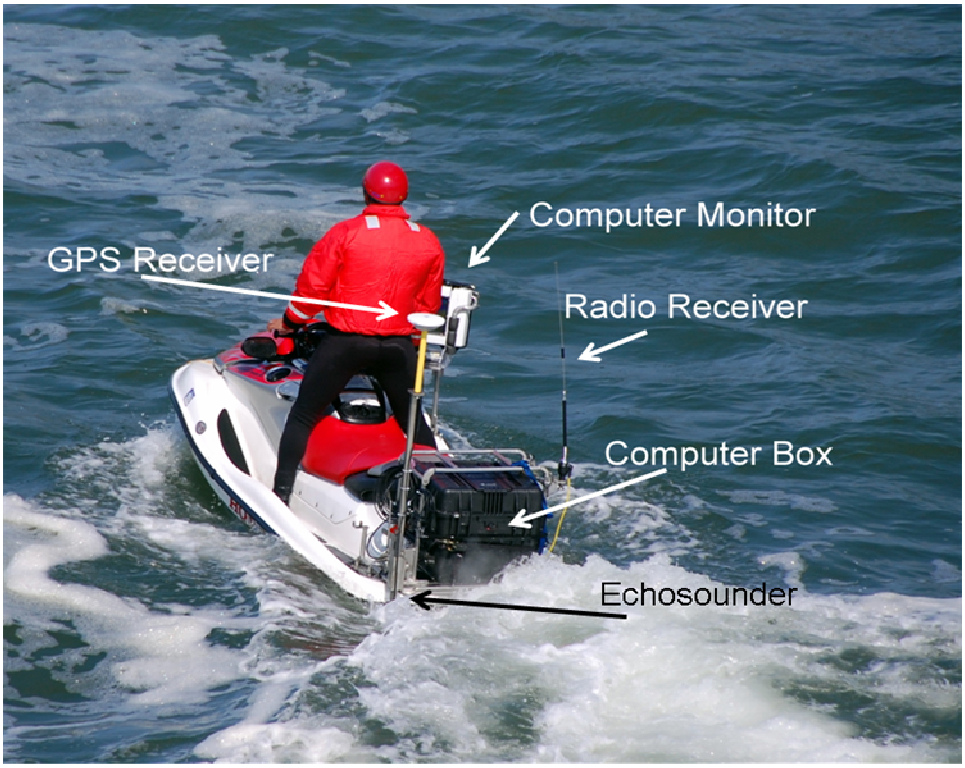

Figure B1) Data acquisition boat and onboard equipment.

Data Processing and Archiving

Our survey data was collected in the horizontal datum Oregon State Plane South, NAD83 (m) and the vertical datum NAVD88 (m) using a geodetic control network setup by Jon Allan of DOGAMI.

Data processing was carried out using the Matlab script *transectViewer.m* developed by Andrew Stevens from the US Geological Survey in coordination with Peter Ruggiero of OSU. This code loads and displays the raw data files and allows the user to navigate through the data and perform appropriate filtering and smoothing. Obvious bad data due to echosounder dropouts or poor returns are easily eliminated from the data record. Various smoothing operations can be applied to eliminate scales of morphological variability below which the user is not interested. Due to the high quality of the raw data in the Reedsport survey only very moderate smoothing was performed (10 point median average, Figure B2).

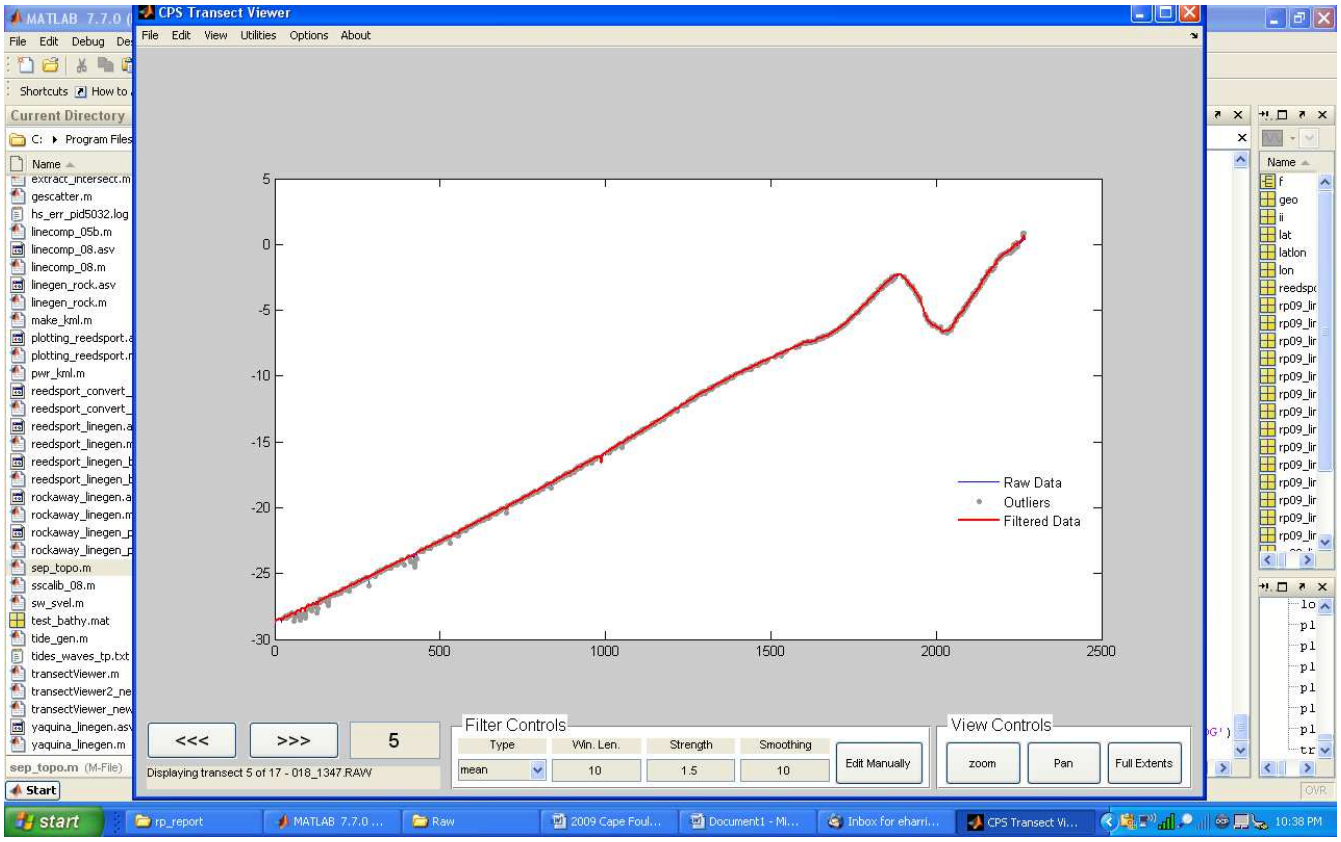

Figure B2) Example profile collected off the coast of Reedsport displayed in transectViewer.

Data Coverage

The surveyed area stretches approximately 13.7*km* alongshore with cross-shore transects extending ~2 *km* offshore (Figure B3). Five lines (# 56, 58, 60, 62, 64) had extended coverage to a distance of 4*km* offshore.

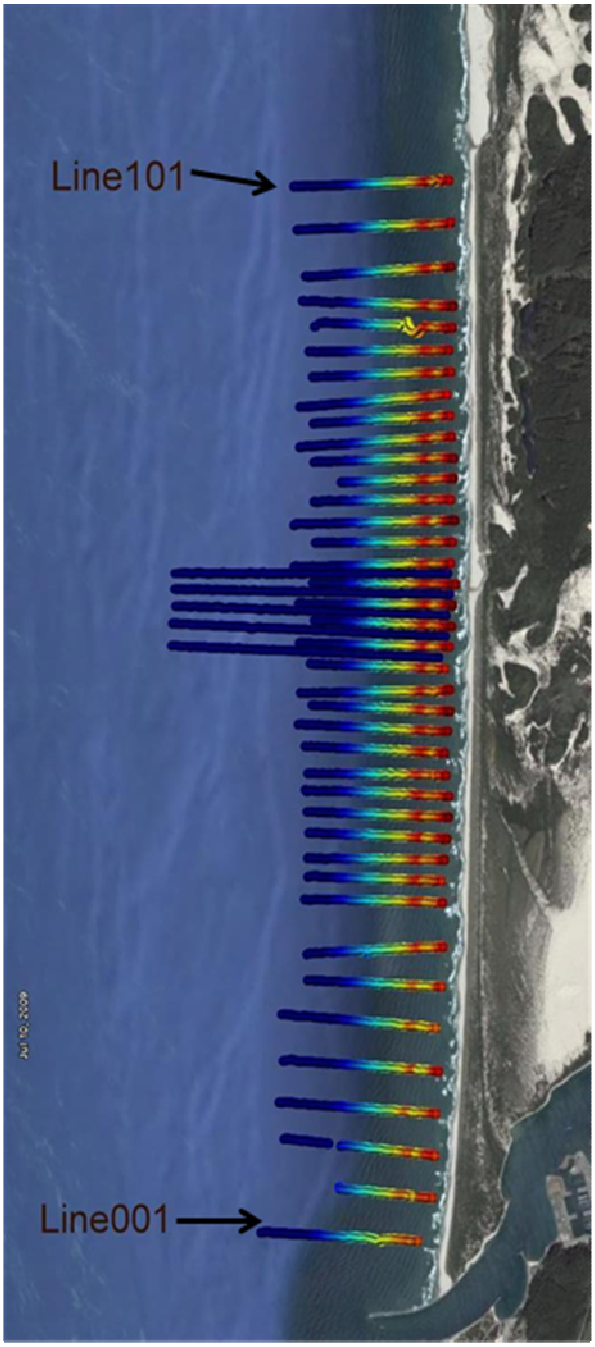

Figure B3) Collected bathymetry transects off the coast of Reedsport.

Reedsport Nearshore Bathmetry

Figure B4 shows a typical nearshore bathymetric profile along the study site. The area is characterized by a single large subtidal sandbar approximately 2 to 3 meters in height and a more subdued intertidal sandbar that was resolved along transects in which the bathymetry transects overlapped with the topographic transects (Figure B4). The subtidal sandbar crest is typically in approximately 2 to 3 m of water (NAVD88) and about 400 meters from the shoreline (~3m contour) while the landward trough is in approximately 5 to 6 m of water.

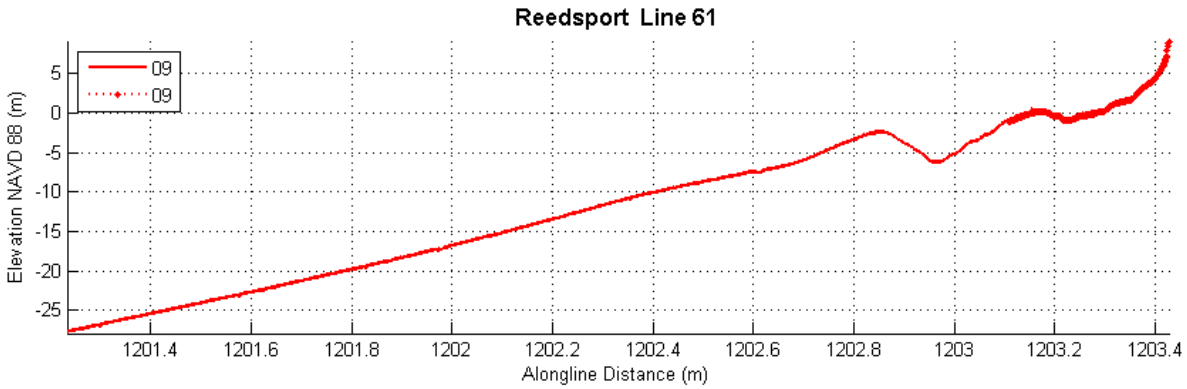

Figure B4) Example cross-shore transect.

Several transects revealed an interesting 'mega-ripple' field in about 8 meter of water offshore of the subtidal sandbar (see Figure B5). These interesting features have length scales on the order of 20 meters and amplitudes on the order of about 20 centimeters.

Deliverables

Reedsport survey data are provided in 2 folders: nearshore_bathymetry and google_earth. Inside the nearshore_bathymetry folder are 45 individual profiles collected by the data acquisition boat. The naming format is rp09_linenumber_b.xyz. Each file is composed of 3 columns of data: Eastings, Northings, and elevation (depth in meters) with reference to Oregon State Plane South, NAD 88(m) in the horizontal and NAVD 88(m) in the vertical.
The google _earth folder contains the 45 bathymetry transects in Google Earth format (.kml). By selecting and opening these individual bathymetry lines, they can be viewed in a Google Earth interface with data points displayed in a color relative to its recorded depth (Figure B3).

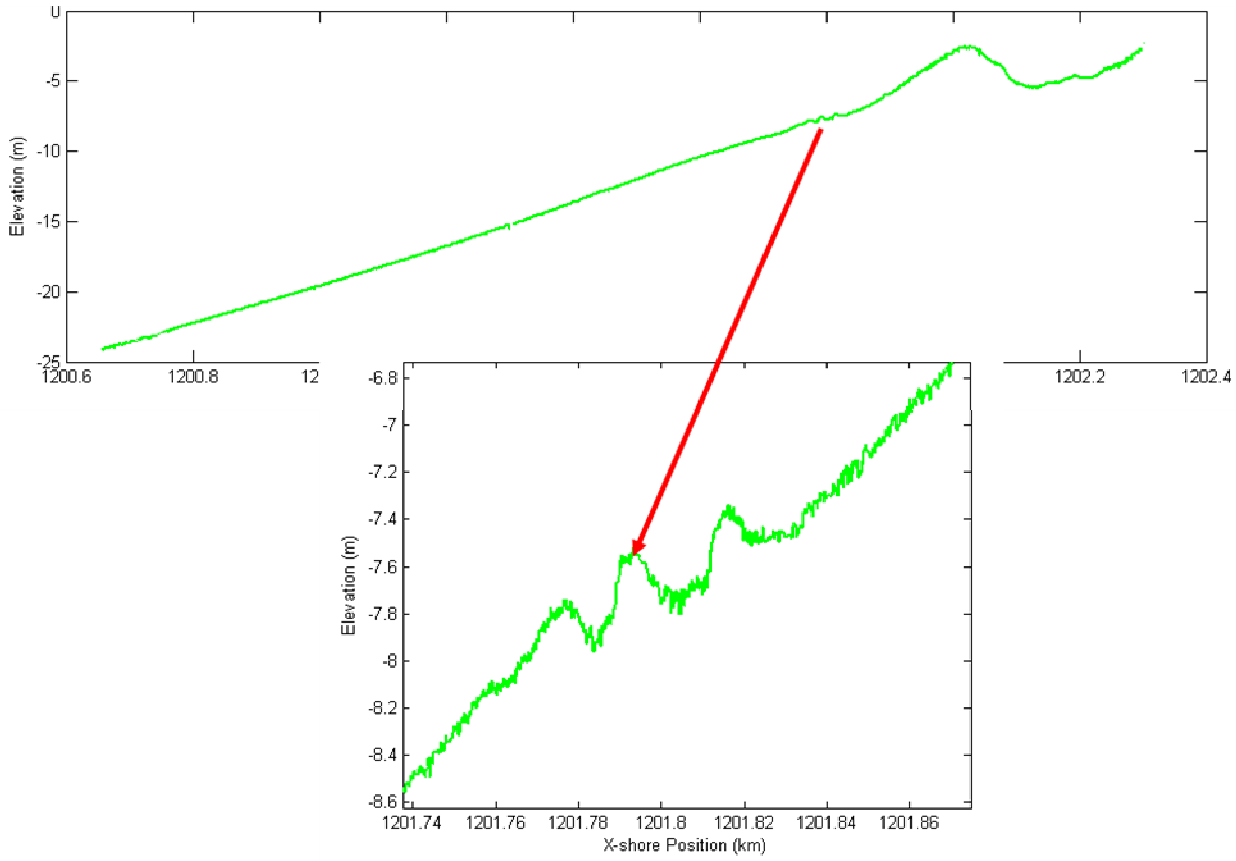

Figure B5) Example cross-shore transect showing 'mega-ripple' field offshore of the subtidal sandbar.

Appendix C

Optical Remote Sensing Results

Rob Holman
Oregon State University

Background:
The installation of wave energy devices offshore in the Reedsport Wave Energy Park will, by definition, remove energy from the incident wave climate. One concern is that this will create a shadow zone that could alter the morphology of the nearshore beaches. To determine the level of this threat, a monitoring program was begun in June, 2009 to measure the base state of the local nearshore environment. This program included traditional GPS survey methods that yield accurate topography and bathymetry at the times of measurement. However, the nearshore environment continually responds to the varying wave energy, so will vary in response to storms, seasons and potentially interannual events. Thus, there is need for more frequent measurements of system changes between surveys. Optical remote sensing through Argus methods provides a low-cost approach for providing such data.

Objective:
The goal of this component of the program was to provide frequent measurements of nearshore morphology variations over a sufficient duration to define a base state, prior to energy device installation. Thus, we hope to define the "typical" nearshore morphology for this site.

Methods:
Morphology is the shape of dominant features in the nearshore topography, typically taken as the position of the shoreline, of offshore sand bars (shoals) and potentially of rip channels. It has been shown that these locations can easily be found by observing the average location of wave breaking patterns in the surf zone. Since waves break in shallow water, zones of concentrated breaking correspond to shoals (or to the shoreline for the final shore break of the waves). These patterns can be observed easily in 10-minute time-exposure images. The method of time exposure imagery was introduced by Lippmann and Holman (1989) and became a core capability in a program of automated observing systems called the Argus Program (fully described in Holman and Stanley (2007)).

Oblique images captured by a typical camera system can in turn be rectified into map images using standard photogrammetric methods (Holland, Holman et al. 1997) if the position of a number of recognizable Ground Control Points (GCPs) are known. Typically one camera will not span the desired field of view, so multiple cameras are used, each pointing to a different part of the beach. Individual images are merged using the same photogrammetry principles. Figure C1 shows an example rectified time exposure image from Reedsport that has been merged from three separate images, each with a different aim point.

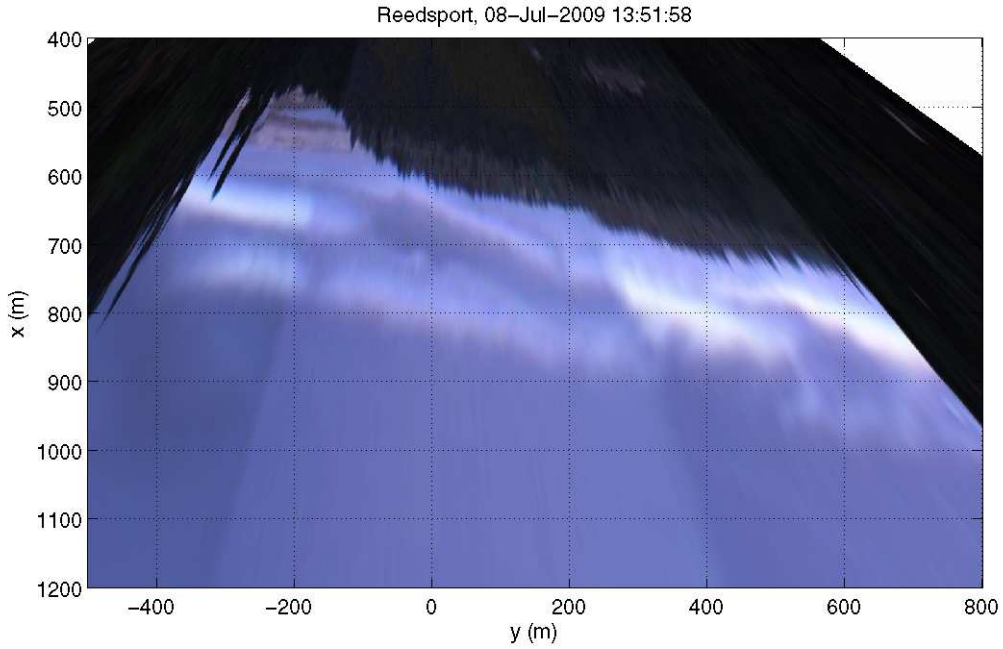

Figure C1. Example merged time exposure image from 8 July, 2009, the first of the monitoring campaign. The shore is at the top of the image and seaward is at the bottom. White bands are regions of preferred breaking corresponding to submerged sand bars. Thus if we look near the center of view (x=100), we see a bar at x=680 and 800m from the cross-shore position of the camera. It was difficult to find a camera location with a full view of the beach, so much of the dry beach is obscured by tall tress (y>125m). However, a narrow section of beach is visible from longshore locations -300 to -100. Note that this image is the composite of three images, each with a different aim point (discernible by the inter-image boundaries).

Normally, Argus stations are fully automated and return imagery every daylight hour of every day. However, they also require power and internet access, luxuries that were not available at this site. Thus, for this application, a portable system was designed consisting of a single camera and a special mounting bracket that forced camera alignment to the three required aim directions. During an initial site visit the mounting post and mount plate were installed and survey locations found of the camera and a number of identifiable objects in each view (GCPs).

Data collection involved hiking out to the site, mounting the camera in the first aim position, then running a laptop program that acquired the first time exposure image (plus snapshot plus an alternate image type). This was repeated for camera positions 2 and 3. Upon returning to the lab, the geometry of each image was determined using a special software tool, then merged rectifications were found using in-house software.

Collections

At the time of writing, data had been successfully collected on five separate days and under a range of wave heights (Table C1).

Date	Hs (m)
07/08/09	1.25
09/17/09	2.02
10/11/09	0.90
11/04/09	0.97
11/17/09	5.94

Table C1. Dates of image collection (left column) and corresponding significant wave heights (right column). Wave measurements were from CDIP buoy 139 (Umqua) in 186m water depth.

The individual merged rectifications are shown in Figures C2a-e. Merged images (and obliques) are on cil-ftp.coas.oregonstate.edu under /ftp/pub/reedy/2009. Obliques (original snaps and time exposures) are listed by camera position, then date. Merged rectifications are under cx (camera 'x') by date. Images differ from each other for three reasons. First, the sand bar location and form changes in response to changing wave energy (this is the natural signal we wish to measure). For instance, the storm bar of September 17 looks very different from the recovered bar system of October 11. Similarly, the offshore positions of the storm bars from September 17 and November 17 are quite different (note that the larger waves reveal the presence of a second offshore sand bar near the bottom edge of this picture. A more extensive rectification (Figure C3) shows the offshore sand bar to be roughly 800 m from the shore.

Second, since bar position is revealed by breaking wave patterns, small waves will reveal only a smaller section of the nearshore morphology (e.g 4 November, when the only breaking patterns are close to the shore and obscured by the trees). Third, tide level variations also determine the locations of breaking. So, despite a similar wave height, the October 11 image show much more structure than the November 4 image due to the lower tide.

Overall, this is very mobile system with multiple sand bars that reach offshore for almost 1,000 m. Bar morphology can be convoluted under prolonged low wave conditions but straighten and move offshore under large storms.

Summary

Time exposure images show the presence and time-varying morphology of the nearshore sand bar system landward of the Reedsport Wave Energy Park. A multiple bar system is present and appears to be quite variable, responding to early winter storms. This variability is part of an annual signal that would require continuing monitoring to characterize. Clear variations in bathymetry are obvious out to about 1,000 m offshore. It is likely that the bar would move further offshore during the upcoming winter stormy season.

The methods used are simple and low cost once set up, depending mostly on the manpower to hike in and carry out the collections. Because they reveal varying amounts of the bar system at different tides and under different wave heights, they are best suited to more frequent sampling. This change should be considered.

References:

Holland, K. T., R. A. Holman, et al. (1997). "Practical use of video imagery in nearshore oceanographic field studies." IEEE Journal of Ocean Engineering **22**(1).

Holman, R. A. and J. Stanley (2007). "The history and technical capabilities of Argus." Coastal Engineering **54**: 477-491.

Lippmann, T. C. and R. A. Holman (1989). "Quantification of sand bar morphology: A video technique based on wave dissipation." Journal of Geophysical Research **94**(C1): 995-1011.

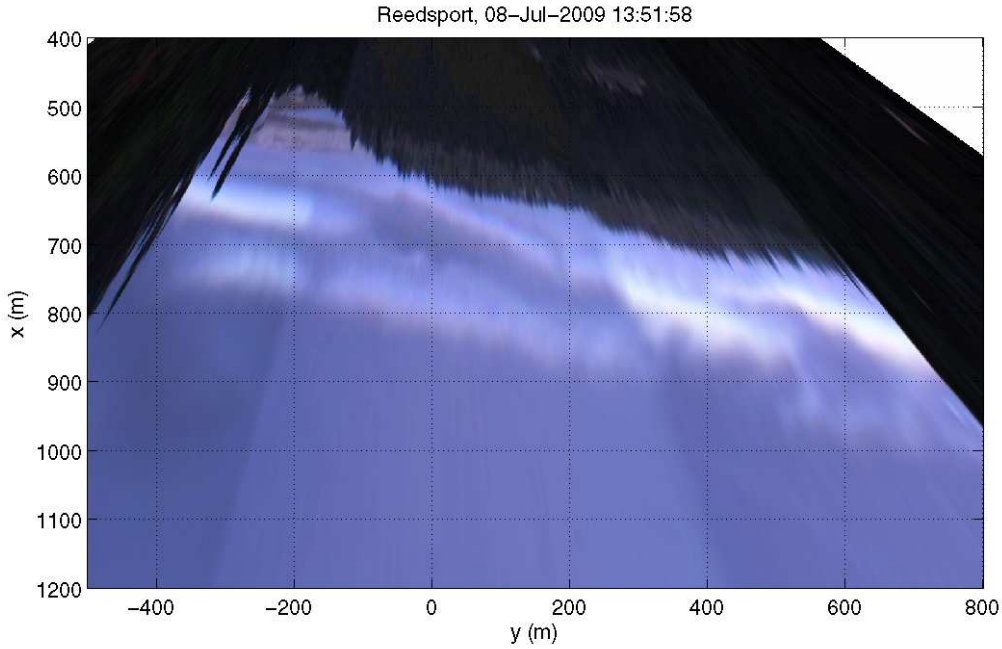

Figure C2a. July 8, 2009 merged rectification.

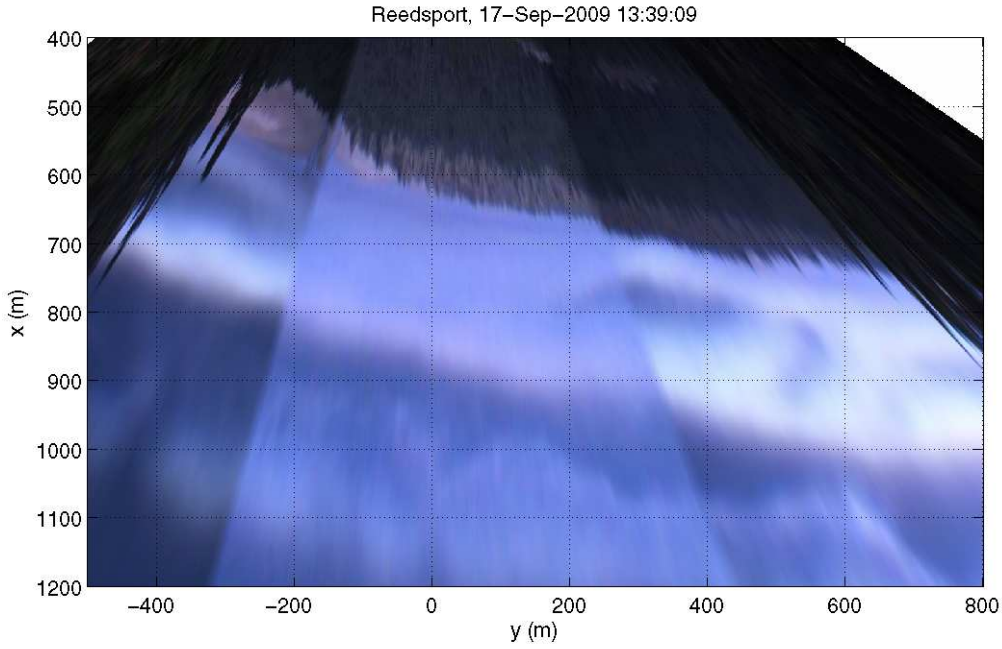

Figure C2b. September 17, 2009 merged rectification.

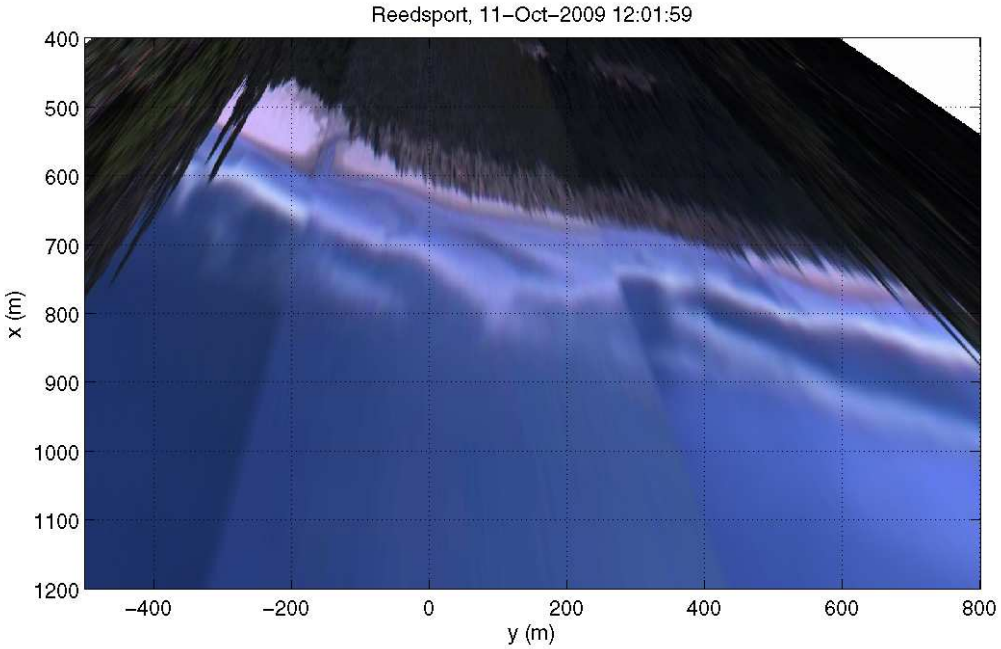

Figure C2c. October 11, 2009 merged rectification.

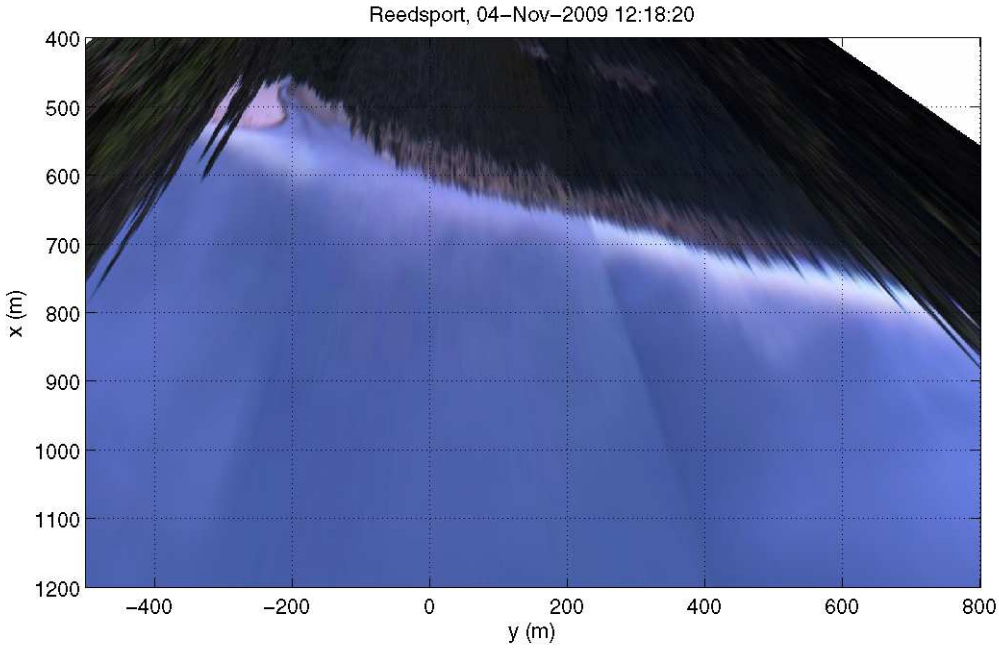

Figure C2d. November 4, 2009 merged rectification.

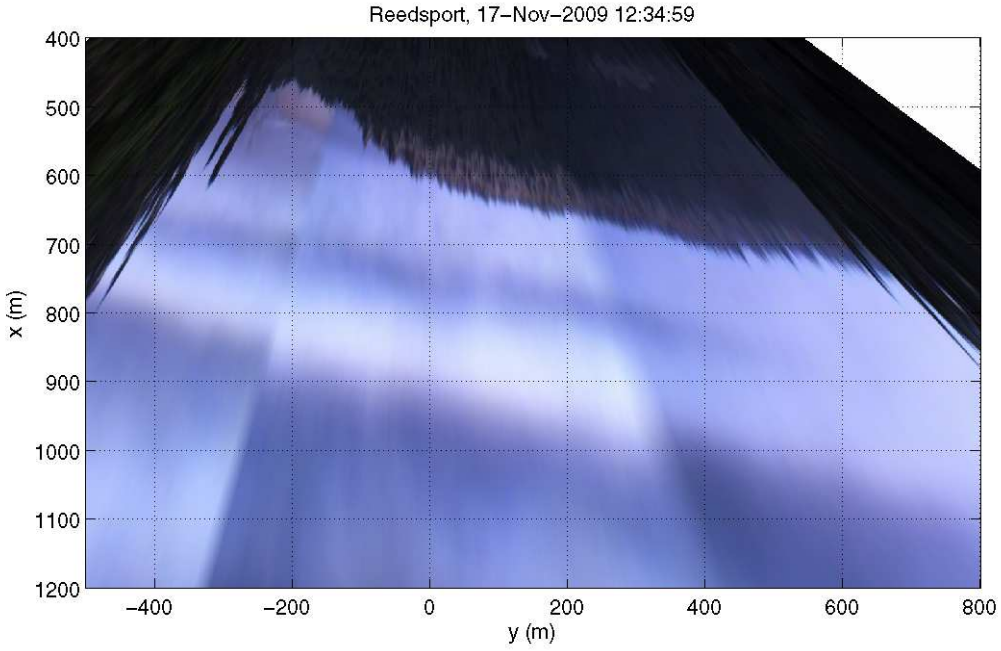

Figure C2e. November 17, 2009 merged rectification.

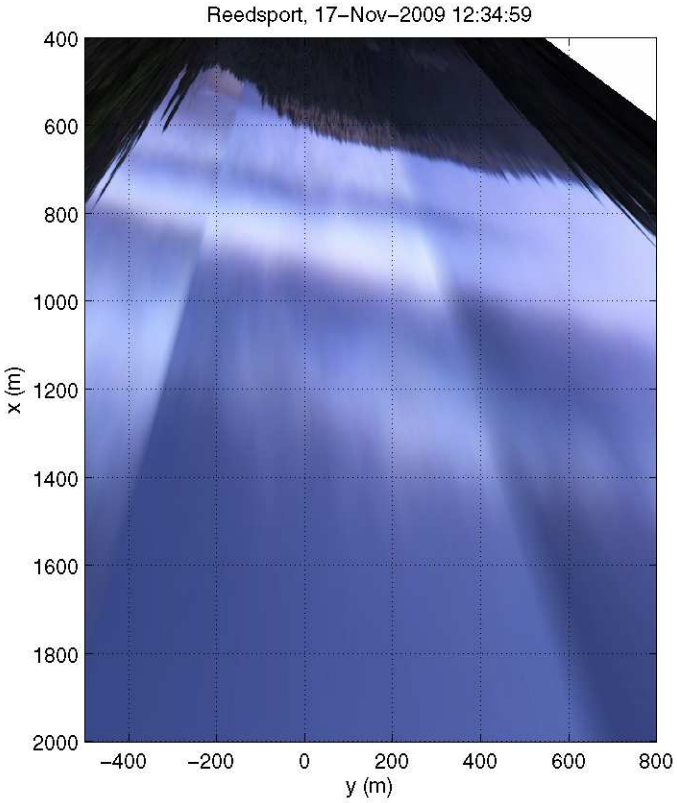

Figure C3. November 17, 2009 merged rectification created on an expanded cross-shore scale to reveal the offshore extent of the offshore sand bar.

Appendix D

Wave Modeling Results

H. Tuba Ozkan-Haller
Oregon State University

Background

Offshore wave conditions along the Oregon coastline are measured at a handful of buoy locations where directional wave information is available. Most of these buoys are located in deep waters and incoming waves undergo changes as they travel from deep water onto the shelf where wave energy conversion arrays are likely to be deployed. These changes can be in the form of wave focusing or defocusing due to the presence of underwater banks, shoals, or canyons. Also, wave dissipation mechanisms such as bottom friction or wave breaking can be at play. Wave models can take into account such processes and produce predictions of the local conditions at the site of a wave energy conversion (WEC) array. Knowledge of local conditions can aid in the design of the devices for the specific local conditions to which they will be subjected and can also provide advance knowledge of wave conditions to power companies once a WEC array is in place.

The work performed herein was geared towards two goals. First, transformation of the wave field from deep water to the site of the buoy deployment was assessed. Second, preliminary predictions about the potential impact of the buoys on the wave field are made. The results are discussed separately below. Note that model code used herein is freely available soft ware and can be obtained through http://www.wldelft.nl/soft/swan/. Input files specific to this work can be obtained through the author.

Wave transformation

The Oregon wave climate is dominated by swells approaching from the southwest and more moderate waves approaching from the west or northwest in the intermediate periods. Using the deep water buoy at NDBC station 46089, we identified several representative wave conditions and show results herein for three of those conditions; namely, short-period waves approaching from the northwest that are typical of a local storm, a moderate swell condition from the west, and a large southwestern swell condition typical of winter storms. Details about these conditions are given in Table D1. Note that we utilize actual measured wave spectra from buoy 46089 as input.

Condition	T_p (sec)	H_s (m)	θ_p (deg)	month
I	6.3	1.7	46 (NW)	July
II	12.9	4.2	-5 (W)	November
III	11.4	5.6	-44 (SW)	January

Table D1: *Characteristics of identified typical wave conditions I, II and III. Noted are peak period (T_p), significant wave height (H_s), and peak angle of incidence measured clockwise from North (θ_p) and the month this condition is most commonly observed.*

We utilized historical bathymetry assembled by the National Geological Data Center (NGDC) and created a model grid that covers a large portion of the Oregon coastline (see Figure D1). The southern boundary of the grid is near the OR-CA border and encompasses 267km in the alongshore direction. The offshore boundary of the grid is located just offshore of the shelf break and covers 86km in the cross-shore direction to the shoreline. There are several bathymetric features contained in the domain that may affect incoming waves. In particular, the Stonewall and Heceta bank systems have the potential of focusing waves near the WEC site when waves approach from the northwestern direction. In this case, the NDBC buoy 46229 is conveniently located in the lee of the banks; hence, comparison of model results with this buoy can lead to verification of refraction predictions. Note that a smaller model domain that would use measured wave spectra at 46229 was also considered, but this would only be advisable if we determine that focusing effects due to the banks are minor.

We determined grid resolution with standard convergence tests and arrived at 200m resolution in the alongshore direction and 100m in the cross-shore direction. The wave spectra are resolved with 5 degree bins in direction and a total of 21 bins in frequency between 0.05Hz and 0.25Hz.

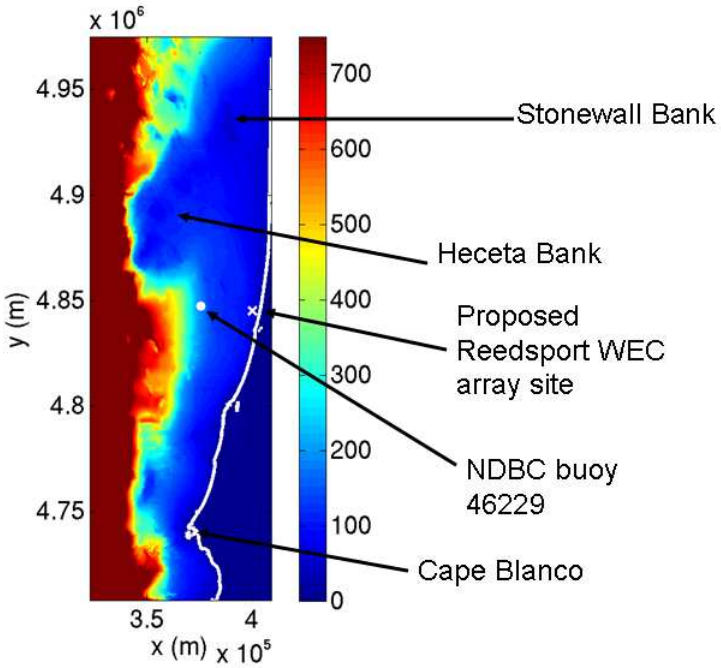

Figure D1: *Water depth within the computation domain. The Stonewall and Heceta Banks, the site of the proposed WEC array site, location of NDBC buoy 46229 and a few other sites are also included for reference.*

Using the bathymetry and incoming spectral information as input, we utilize the spectral wave transformation model SWAN (Simulating Waves Nearshore) for the identified representative wave cases and estimate the wave field in the entire domain. NDBC station 46229 at approximately 190m depth is used as a validation point, and we also determine the expected wave spectra at the proposed WEC array site.

Figure D2 shows results for the three identified cases, Figure D3 shows the evolution of the wave height across the shelf at an alongshore position that corresponds to the position of buoy 46229. For

Case I involving moderate short-period waves from the NW, waves evolve minimally over the shelf. This is because the wave period is relatively short (~6sec); and these short waves are still in deep water at the water depth of the banks. In contrast, the longer period waves associated with Cases II and III (~12sec) are affected by the presence of the banks. However, because of the primary direction of propagation, these effects are not significant near the site of the proposed WEC array. For Case III when waves approach at high angles from the south, Cape Blanco causes a shadow that results in reduced wave height at the proposed WEC site. The predicted reduction is also observed by buoy 46229 (see Figure D3). The waves that reach the WEC site under these circumstances have refracted around Cape Blanco and therefore display lower angles of incidence compared to locations further offshore (see Figure D3). In contrast, waves associated with Case II does not experience significant refraction at the transect corresponding to the WEC array site (see Figure D3). This is because these waves approach almost directly from the west and are therefore already perpendicular to the depth contours. For Case I, the period of the waves is very short, so the waves do not feel the bottom until quite shallow depths and wave angle reduction due to refraction processes is confined to a small area near the shore.

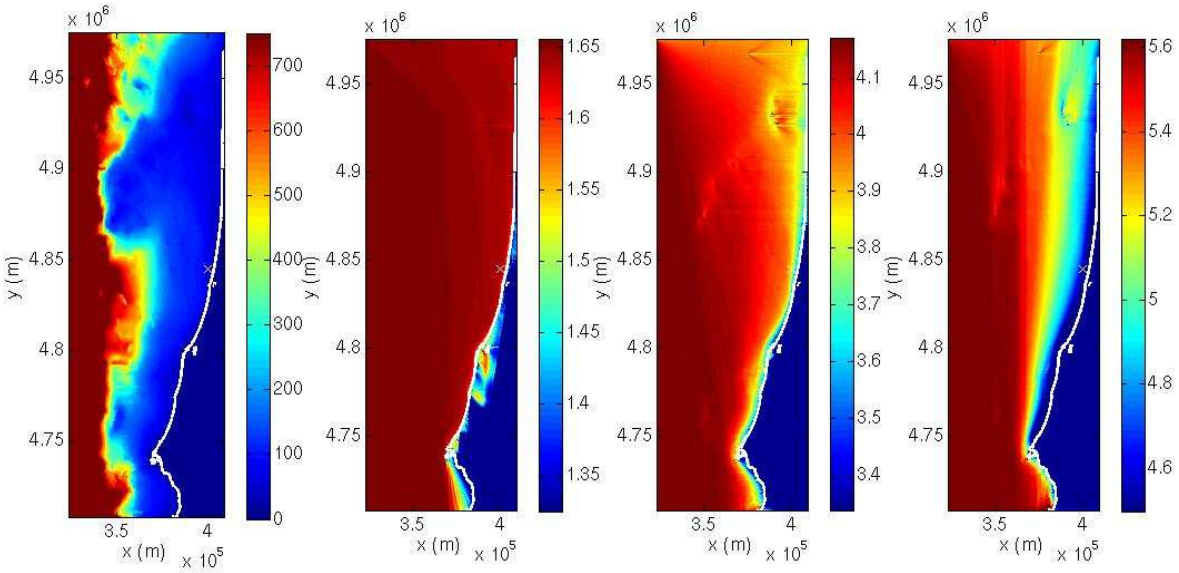

Figure D2: *panels left to right – water depth, wave height for wave conditions I, II and III (see Table D1). A right-handed coordinate system is used with x pointing east and y pointing north. Positions are indicated in northings and eastings in meters.The shoreline contour is outlined in white. The location of the proposed Reedsport WEC array is indicated with a white cross (near y=4.85×10^6m). The color scale is indicated next to each panel. Note that it is different for each panel. The wave height scales indicate 20% variability around the offshore wave height to highlight the expected variability over the continental shelf.*

Comparison between predicted and observed wave heights near the WEC array site for the example cases discussed so far is favorable (see Figure D3). Longer term simulations over several months were also carried out (see Figure D4) and suggest that the wave model performs generally well, but there are distinct periods of discrepancy between predictions and observations. The causes for these discrepancies are currently not known but may be related to inaccuracies in the historical shelf

bathymetry (which are based on shelf surveys that are not recent), inaccuracies in the input wave conditions, or model physics that isn't represented well.

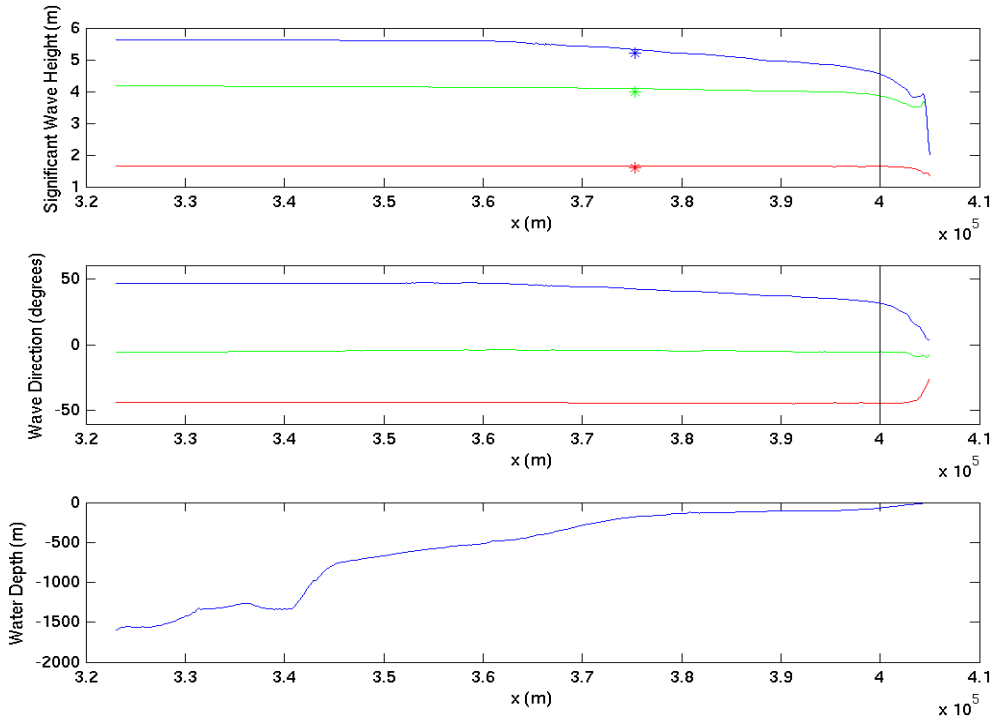

Figure D3: *Wave height (upper panel), wave angle (middle panel) and bathymetry (lower panel) along a cross-shore transect located at y=4847500m (which corresponds to the alongshore position of buoy 46229). The lines indicate results for waves from the NW (case I, red), from the W (case II, green) and from the SW (case III, blue). Symbols indicate measured wave height at buoy 46229.Wave angle is reported as 0 degrees if wave approach from the west. Waves approaching from the south (north) correspond to positive (negative) angles. Finally, the location of the proposed WEC array site is indicated with a black vertical line in each of the subplots.*

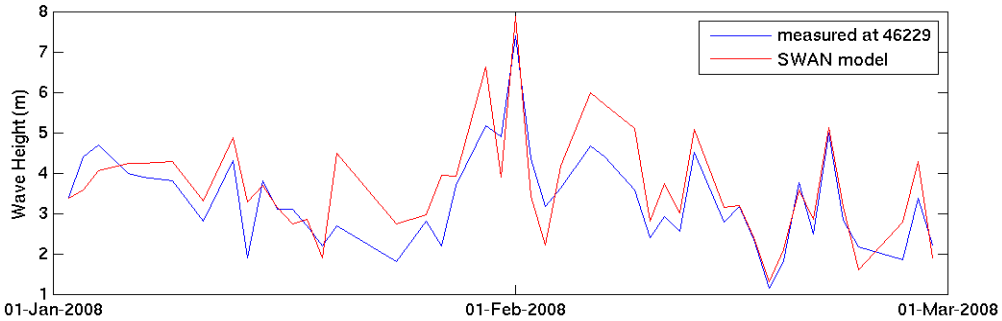

Figure D4: *Comparison between predicted (red) and observed (blue) wave height at NDBC buoy 46229 over 2 months of simulations.*

The model simulations also provide detailed information about the expected wave spectra conditions at the site of the proposed WEC array. For the three example cases discussed herein, the wave spectra are shown in Figure D5. As a result of this work a wave model domain has been setup that adequately addresses wave modifications over features (banks, capes, canyons) on the shelf. Validation of the model results will be ongoing as part of the wave forecasting work that is part of the NW National Marine Renewable Energy Center (NNMREC) and also as part of a new NOAA Sea Grant project (beginning February 2010) related to the prediction of waves along the entire OR coast.

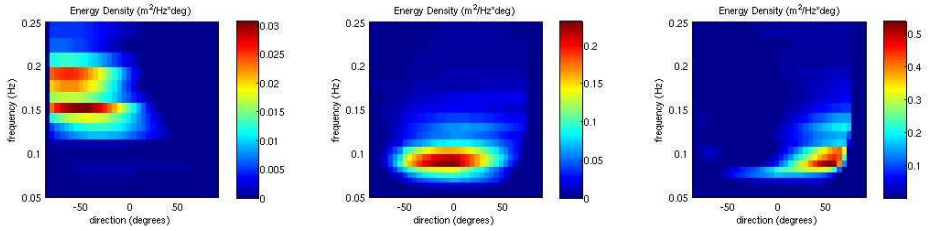

Figure D5: *Wave energy spectrum at the proposed location of the WEC array. Panels left to right at for Cases I, II and III. Values for the angles in these plots are relative to waves approaching directly from the W (indicated as 0 degrees). Positive (negative) angles correspond to waves approaching from the south (north).Color scales for each panel are indicated. Note that they differ for each case.*

Potential impact of buoys on wave field

A second goal of this work has been to make preliminary predictions about the potential impact of WEC buoys on the wave field. A detailed wave-structure interaction model that accounts for the detailed mooring characteristics of the buoys as well as their movement is beyond the scope of this project. Such a model would also require very large computational resources, so that the assessing an array of devices would not be feasible. Our approach has, therefore, been to use a high resolution sub-domain and represent the buoys empirically as stationary structures that absorb a certain amount of wave energy. For this purpose, we used a test case that accurately represents the conditions at the proposed WEC array site (e.g. water depth, distance from shore, slope of shelf at this location) and used very high spatial resolutions so that we could represent individual buoys as stationary structures in the model domain. We experimented with cylindrical or straight structures. Their size and energy absorption characteristics are then the empirical coefficients that can be altered to produce shadowing behavior similar to an actual wave buoy. Note that the behavior of each kind of device may be different, and detailed wave-structure modeling of the type discussed above will aid in the calibration of the coefficients. Such detailed modeling is planned as part of the NNMREC. However, direct observations of the shadow zone for a device are even more important, both to validate any detailed wave-structure interaction model, and also to calibrate coefficients in the model setup here.

Results from our empirical modeling for an array of 5 WECs are shown in Figure D6. The size and severity of the predicted shadow regions is a direct function of the size of the structures and their level of energy absorption. The values for these characteristics need to be calibrated with observations, which are not currently available. Therefore, the results shown herein are only a suggestion about the kind of wave height variability that may exist in the lee of an array of WECs. In this case (Figure D6), ~15% variability in the wave height is predicted directly in the lee of the array.

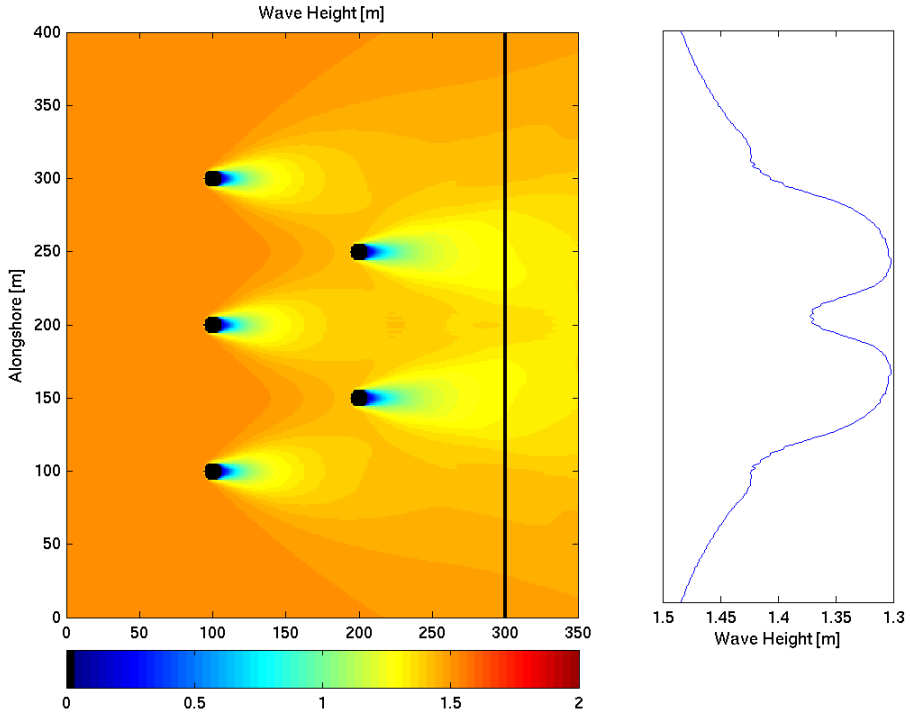

Figure D6: *Potential effect of 5 WECs arranged in an array. The left panel shows wave height in a region immediately surrounding the array. A transect at the cross-shore position of 300m is indicated. The right panel shows the wave height along this transect.*

The resulting variability in the wave height near a shoreline that is about 4km shoreward of the array is depicted in Figure D7. In the absence of a WEC array waves propagating towards shore experience a small decrease in wave height as they start feeling the presence of the bottom, then go on to shoal as the wave speed slows down and finally break near the shoreline. In this case, the surf zone is only ~100m wide. Next we carried out simulations that included the WEC array that we already examined in Figure D6. The array was placed about 4km from the shoreline. These simulations suggest that the small-scale variability (at the length scale of the distance between the structures) diffuses within about 1km of the array. The remaining larger-scale depression in the wave height persists to the shoreline, but at a reduced magnitude of about 3%. Calibration and validation of these results hinges on observations of the wave heights in the vicinity of an actual device.

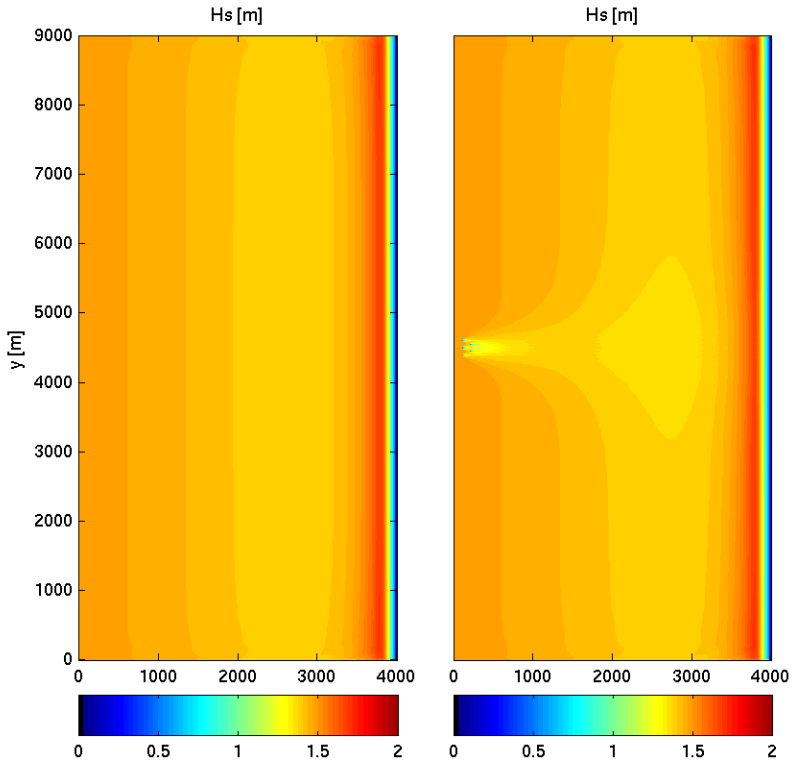

Figure D7: *(left panel) Wave height over a planar shelf with no WEC devices. Waves travel from the offshore boundary on the left-hand-side towards shore.*
(right panel) Wave height including the effect of a WEC array placed

Appendix E

In-situ Observations and Marine Radar Wave Observations

Jack Barth and Merrick Haller
Oregon State University

In-situ observations

A pair of in-situ sensors were deployed at the Reedsport site. The first was a Nortek Acoustic Wave and Current (AWAC) instrument and was deployed in a bottom frame shoreward of the wave energy site at the 41-m isobath (43° 45.080' N, 124° 13.195' W). The second was a Datawell Directional Waverider surface buoy, which was deployed offshore of the wave energy site at the 90-m isobath (43° 45.187' N, 124° 16.047' W). Both of these sensors were on-loan to the project from Dr. Annette Von Jouanne and the group at the Wallace Energy Systems & Renewables Facility (OSU).

The installation and recovery of the instruments were done from the Charter Vessel Miss Linda operating out of Coos Bay, OR. The AWAC was deployed on September 18, 2009, and recovered from the same vessel on December 2, 2009, a total of 75 days, longer than the proposed 2-month deployment period. In addition to measuring significant wave height and directional wave spectra, the AWAC also measured vertical profiles of horizontal currents. The vertical stratification of the water column at this 41-m site was measured using temperature sensors deployed near the surface on the AWAC marker buoy and near the bottom on the AWAC bottom frame. The temperature sensors were programmed to record for two months, hence they stopped recording before the AWAC was recovered.

The deployment of the Waverider was slightly delayed (October 8, 2009) because it needed extensive repair after being stored in non-working condition after its last use in the ocean. The Waverider measures directional wave spectra, but not ocean currents. The Waverider data, including its GPS location, were continuously transmitted to, and stored on, an off-network shore station using a radio link. Unfortunately, the Waverider broke free from its mooring on October 23, 2009, just 15 days into the planned 3-month deployment. Since waves and currents were well below the design specifications for the Waverider mooring, we suspect the buoy broke free after being hit by a vessel. Fortunately, the instrument was recovered off Cascade Head, OR (near 45° 0' N) on December 10, 2009, and is still in good working order.

The wave, current, and temperature data from the two in situ sensors are presently undergoing quality control and calibration. The data are scheduled to be archived on the Oregon Coastal Ocean Observing System (OrCOOS, a sub-regional partner of the Northwest Association of Networked Ocean Observing Systems, NANOOS) data server and web site (http://www.orcoos.org). However, an initial analysis is presented here. Time series of significant wave height and water temperature from the AWAC are shown in Figure E1, along with the closest buoy-measured wind data (NDBC 46050, twenty miles offshore of Newport, OR) to show the strength and direction of the winds which generate local waves. Also, for comparison significant wave heights measured by NDBC Station 46229 (Umpqua Offshore), maintained by the Coastal Data Information Program (CDIP 139) of Scripps Institute of Oceanography (43.769 N 124.551 W). This station is located on the 187-m isobath and is also a Datawell Waverider.

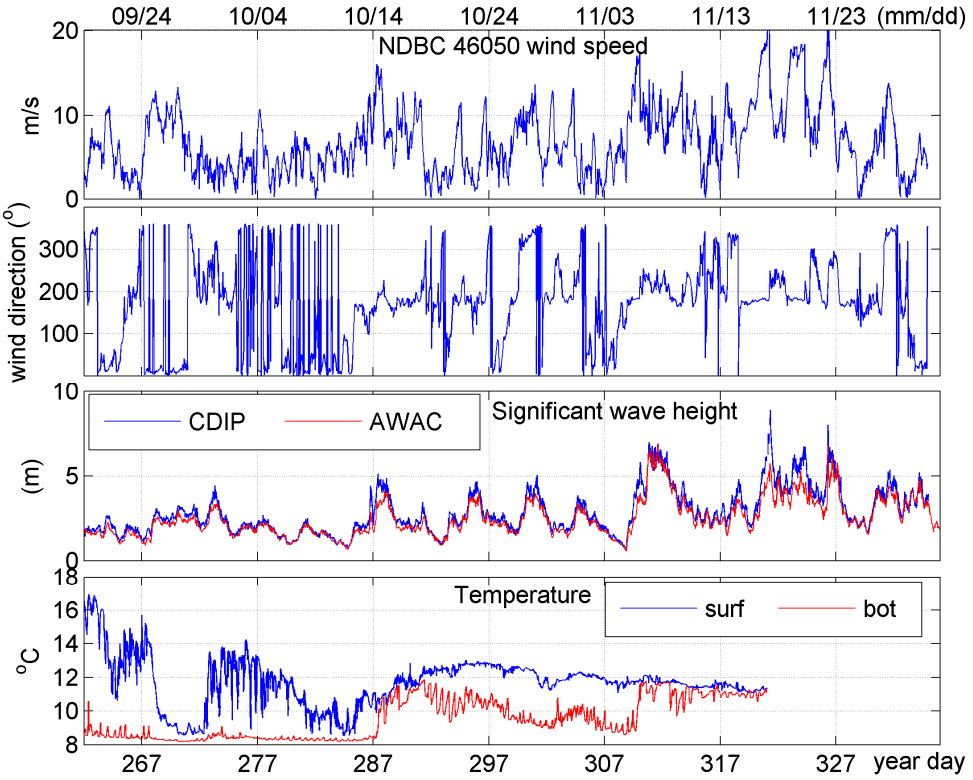

Figure E1: (top two panels) Winds measured at the NOAA NDBC Buoy 46050. (middle) Time series of significant wave height measured by AWAC at the 41-m isobath (red) and by CDIP 139 at the 187-m isobaths (blue). (bottom) Temperature measured at the surface (blue) by the AWAC marker buoy and at the bottom (red) on the AWAC deployment frame.

Wave data time series from the shorter duration Waverider deployment are compared with the other sensors in Figure E2. From our first look at the data we can notice two things. First, the time series of wave height and peak period from the AWAC and Waverider closely track each other. This was expected and confirms that, in the absence of wave energy converters at the Reedsport site, there are no significant shoaling/refraction effects occurring across the wave energy site (i.e. between the 90-m and 41-m isobaths). The in situ data from Reedsport also well track the data from the offshore CDIP station; however, there are some interesting differences noted around year days 286-288 (Oct. 13-15, 2009).

The second aspect of note can be seen in Figure E3. There we isolate the data from year days 286-288 and demonstrate the relationship between wave direction and the wave height observed off Reedsport. The top panel of Figure E3 indicates that during year days 286.5-288 the wave heights measured at the Reedsport site are substantially lower than those measured at the offshore CDIP. We note that during these days there was a storm blowing from the south (Figure E1), offshore wave heights reached 4-5 m and, most importantly, wave directions switched to the south (waves arriving from ~200 degN at the CDIP). Hence, these data suggest that wave refraction and shadowing effects from Cape Blanco to the south are reducing the wave heights at the Reedsport site during these conditions. This effect was also discussed in Appendix D.

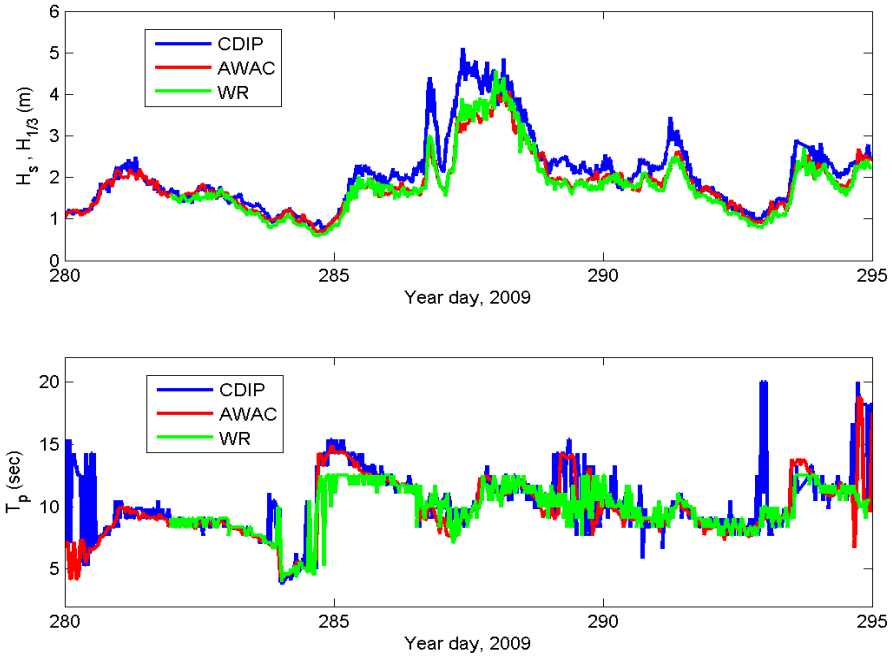

Figure E2: (top) Time series of significant wave height from the Waverider at the 90-m isobaths (green), AWAC (red), and by CDIP 139 (blue). (bottom) Time series of peak wave periods measured by those same instruments.

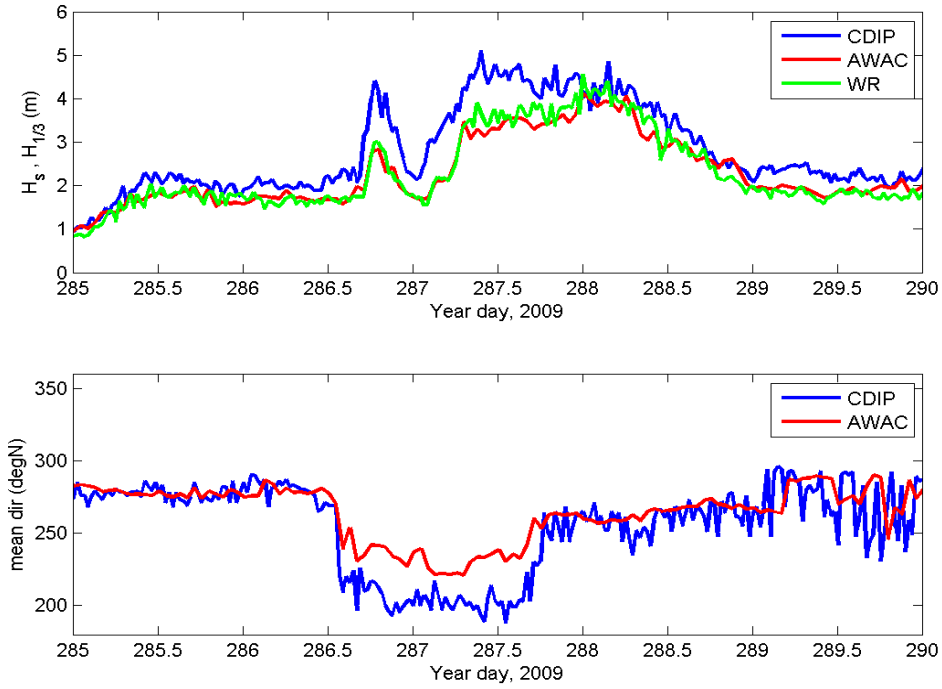

Figure E3: (top) Portion of significant wave height time series from the Waverider (green), AWAC (red), and by CDIP 139 (blue). (bottom) Time series of mean wave directions as determined by CDIP 139 (blue) and AWAC (red).

Wave observations with Marine Radar

Additional wave observations were collected using the marine radar system aboard the C/V Miss Linda during the instrument deployment cruises (Sept. 18 and Oct. 8, 2009). The radar aboard the Miss Linda is a 4 kilowatt Furuno with a 3.9 degree beam width radome antenna. Under this OWET project the radar display was upgraded so that digital radar images could be captured while underway using a VGA to USB conversion device. Figure E4 shows a single frame capture from the radar display that is overlain a Google Earth image of the Reedsport area. As this image was captured the vessel (and radar) were positioned at the center of the image approximately 1 mile offshore. A subset image is also shown in Figure E4 to help illustrate the wave signal in the images that will be analyzed.

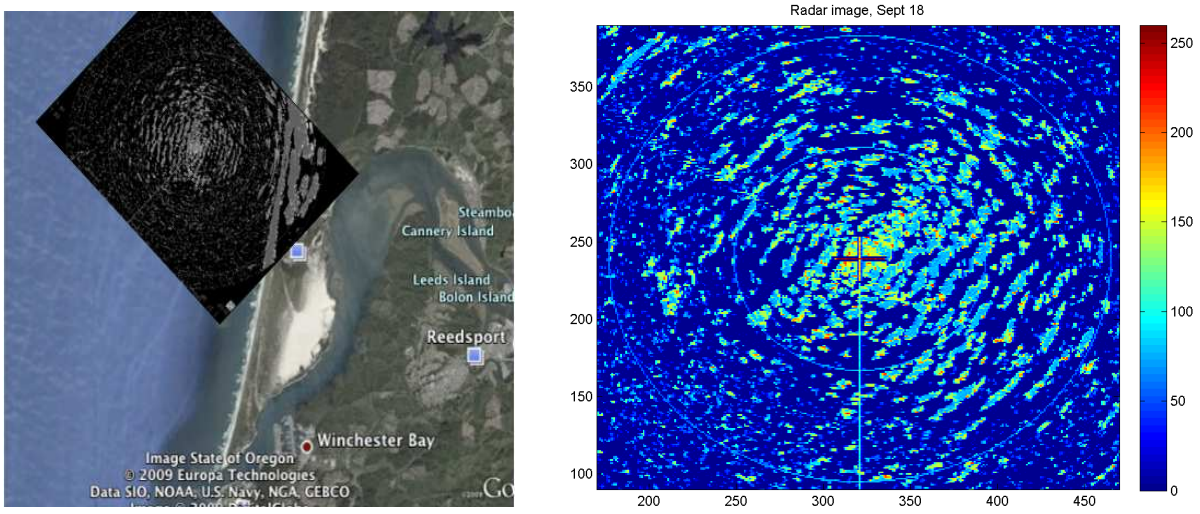

Figure E4: (left) Single radar snapshot overlain a Google Earth image of Reedsport area. (right) Subset radar image, colors represent intensity of the radar return.

The raw radar data shown in Figure E4 were recorded in image (.jpg) files (480 x 650 pixels) and then processed in Matlab to extract wave spectra. The bright linear features represent wave crests. The collected radar time series were approximately 10 minutes in duration and consist of 768 images with an image sampling rate of ~1.28 Hz.

The purpose of these radar collections were proof-of-concept in nature in order to demonstrate shipboard wave observing capabilities while under way. In the future, once wave energy converters are deployed at the Reedsport site, radar can be used to investigate detailed wave scattering and attenuation processes induced by an array of devices. With the data collected herein we have performed basic spectral analysis. An example radar-derived wave spectrum from September 18th 2009 (year day 261) is shown in Figure E5 along with the spectrum measured by the CDIP station. Also listed are the peak wave periods derived from the radar images, the AWAC, and the CDIP station, and they are all in close agreement within their respective resolutions.

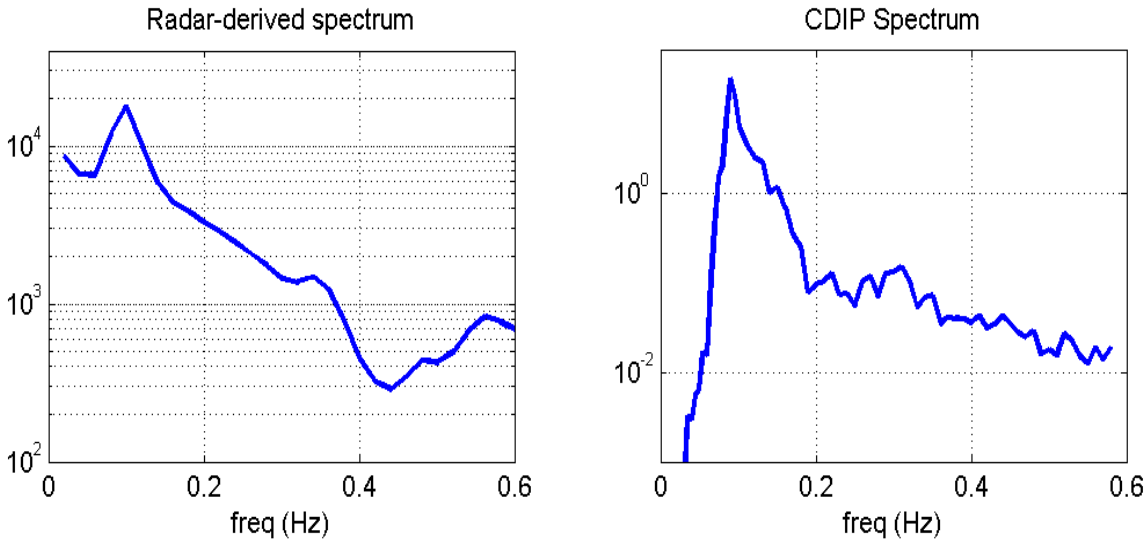

Figure E5: (left) Radar-derived wave spectrum, arbitrary units (right) corresponding wave spectrum from the offshore CDIP station, Sept 18 1200PST. Peak wave periods observed at this time were Tp = 9.96s (radar), 11.11s (CDIP), and10.91 (AWAC).